Immunity
Article

Type I Interferon Inhibits Interleukin-1 Production and Inflammasome Activation

Greta Guarda,[1,6] Marion Braun,[2,6] Francesco Staehli,[1] Aubry Tardivel,[1] Chantal Mattmann,[1] Irmgard Förster,[3] Matthias Farlik,[4] Thomas Decker,[4] Renaud A. Du Pasquier,[5] Pedro Romero,[2] and Jürg Tschopp[1,*]
[1]Department of Biochemistry, University of Lausanne, 1066 Epalinges, Switzerland
[2]Ludwig Institute for Cancer Research, 1011 Lausanne, Switzerland
[3]Institut für umweltmedizinische Forschung gGmbH, University of Duesseldorf, 40225 Duesseldorf, Germany
[4]Max F. Perutz Laboratories, Department of Genetics, Microbiology and Immunobiology, University of Vienna, 1030 Vienna, Austria
[5]Service of Neurology, Department of Clinical Neurosciences and Service of Immunology, University Hospital of Lausanne, 1011 Lausanne, Switzerland
[6]These authors contributed equally to this work
*Correspondence: jurg.tschopp@unil.ch
DOI 10.1016/j.immuni.2011.02.006

SUMMARY

Type I interferon (IFN) is a common therapy for autoimmune and inflammatory disorders, yet the mechanisms of action are largely unknown. Here we showed that type I IFN inhibited interleukin-1 (IL-1) production through two distinct mechanisms. Type I IFN signaling, via the STAT1 transcription factor, repressed the activity of the NLRP1 and NLRP3 inflammasomes, thereby suppressing caspase-1-dependent IL-1β maturation. In addition, type I IFN induced IL-10 in a STAT1-dependent manner; autocrine IL-10 then signaled via STAT3 to reduce the abundance of pro-IL-1α and pro-IL-1β. In vivo, poly(I:C)-induced type I IFN diminished IL-1β production in response to alum and *Candida albicans*, thus increasing susceptibility to this fungal pathogen. Importantly, monocytes from multiple sclerosis patients undergoing IFN-β treatment produced substantially less IL-1β than monocytes derived from healthy donors. Our findings may thus explain the effectiveness of type I IFN in the treatment of inflammatory diseases but also the observed "weakening" of the immune system after viral infection.

INTRODUCTION

In response to cytosolic viral invasion, activation of intracellular RIG-I-like receptors triggers interferon-β (IFN-β) production (Meylan et al., 2006). Specialized immune cells can also produce type I IFN (both IFN-α and IFN-β) in response to extracellular stimuli of viral or bacterial origin by toll-like receptor (TLR) engagement. For example, conventional dendritic cells (cDCs) and macrophages produce IFN-α and IFN-β in response to TLR3 and TLR4 stimulation. In addition, plasmacytoid dendritic cells (pDCs), a specialized type of IFN-producing antigen-presenting cell (APC), can also produce type I IFN in response to TLR-7 and TLR-9 ligands (Meylan et al., 2006; Stetson and Medzhitov, 2006).

Type I IFNs bind to a common receptor, the type I IFN receptor (IFNAR), composed of two subunits (namely IFNAR1 and IFNAR2), which are associated with the Janus kinases (JAKs) tyrosine kinase 2 (TYK2) and JAK1. Activation of TYK2 and JAK1 causes phosporylation of signal transducers and activators of transcription-1 (STAT1) and STAT2, leading to the formation of a trimeric complex composed of phosphorylated STAT1 (pSTAT1), pSTAT2, and IFN regulatory factor 9 (IRF9). This complex translocates to the nucleus where it binds to IFN-stimulated response elements (ISREs), motifs present in promoters and enhancers of interferon-stimulated genes (ISGs), to regulate transcription. Moreover, pSTAT1 homodimers, STAT3, and STAT5 can play a role downstream of IFNAR (Platanias, 2005).

Particular attention has been paid to the anti-inflammatory effects exerted by type I IFN, demonstrated by two lines of evidence (Billiau, 2006; Theofilopoulos et al., 2005). First, patients recovering from a primary viral infection are often more susceptible to secondary infection. In such circumstances, an immunosuppressive role of α- and β-IFNs was suggested by several reports (Decker et al., 2005; Jensen et al., 1992; Shahangian et al., 2009). Second, a number of studies show the effectiveness of this family of cytokines in reducing inflammation in different experimental settings and, most importantly, type I IFN is successfully used in the clinic, not only for the treatment of diseases of viral origin but also for the management of diseases such as multiple sclerosis (MS) (Barkhof et al., 2007; Billiau, 2006; Comi et al., 2001; Giovannoni and Miller, 1999). For patients suffering from MS in the relapsing-remitting phase (RR-MS), IFN-β markedly attenuates the course and the severity of the disease, contributing to the maintenance of the blood-brain barrier integrity and reducing the occurrence of relapses. More recently, IFN treatment has also been successfully used for patients suffering from familiar Mediterranean fever (FMF) and from Behcet's syndrome, two inflammatory disorders linked to IL-1 overproduction (Kötter et al., 2004; Tweezer-Zaks et al., 2008).

IL-1β and IL-1α are two potent proinflammatory cytokines, which share a common IL-1 receptor (IL-1R). IL-1β is synthesized as an inactive precursor, pro-IL-1β, which requires cleavage by caspase-1 in order to attain its active form (indicated as p17, because of its molecular weight of 17 kDa), whereas

IL-1α does not require processing for activity (Mosley et al., 1987). Caspase-1 activation is accomplished within a protein complex known as "inflammasome," which comprises, beside caspase-1 and its substrate pro-IL-1β, a sensor protein (Martinon et al., 2002). To date, four different sensors able to induce inflammasome platform assembly have been identified, NLRP1b, NLRP3, IPAF (NLRC4), and AIM2, which trigger the formation of the inflammasome in response to distinct stimuli (Martinon et al., 2009; Schroder et al., 2009).

Though IL-1β contributes to the control of several pathogenic infections, such as *Salmonella typhimurium* and *Candida albicans* (Bellocchio et al., 2004; Gross et al., 2009; Lara-Tejero et al., 2006), an excessive production of this cytokine has been associated with several autoinflammatory and/or autoimmune conditions such as FMF or cryopyrin-associated periodic syndromes (McDermott and Tschopp, 2007).

Despite the growing use of type I IFN in the clinic, the mechanisms underlying its protective effects in autoimmune and inflammatory disorders are still poorly understood. Some reports propose a role for IFN-β in altering integrin and matrix metalloproteinase expression or activity, thereby reducing leukocyte infiltration to the site of inflammation (Billiau, 2006). IFN-β was also shown to alter the production of several cytokines involved in T cell polarization or in inflammation, including IL-1β (Billiau, 2006; Coclet-Ninin et al., 1997; Huang et al., 1995; Masters et al., 2010; Zang et al., 2004). However, the mechanisms explaining this observation and their relevance to the clinic have never been thoroughly assessed. Specifically, the effects of type I IFN on inflammasome-dependent cytokine maturation have not been investigated. We therefore examined the possible role of type I IFN in controlling inflammasome activity and IL-1 production, which might account for both the efficacy of IFNs in therapeutic settings and the immunosuppressive effects of this cytokine after viral infection. We indeed found that type I IFN strongly suppressed IL-1 production. This was due to STAT1-dependent inhibition of NLRP3 and NLRP1 inflammasome activity. In addition, in bone marrow-derived macrophages (BMDMs), type I IFN enhanced the production of IL-10, which in turn decreased the levels of pro-IL-1α and pro-IL-1β. In vivo, pro-IL-1β induced by aluminum salts and *Candida albicans* was suppressed by type I IFN, rendering mice highly susceptible to *Candida* infection. Moreover, monocytes derived from IFN-β-treated MS patients showed decreased IL-1β production in response to inflammasome stimulation, recapitulating the suppressive effects of type I IFN observed in vitro and in vivo in the murine model.

RESULTS

IFN-β Suppresses Both Pro-IL-1β Availability and IL-1β Maturation

To assess the anti-inflammatory effects of type I IFN on IL-1 production, we incubated BMDMs for 12 hr with IFN-β. Cells were then primed with lipopolysaccharide (LPS) for 4 hr in order to induce pro-IL-1β synthesis and stimulated with alum to activate IL-1β maturation via the NLRP3 inflammasome. We found that IFN-β blocked the secretion of IL-1β by suppressing the activation of both caspase-1 and the intracellular pro-IL-1β pool (Figure 1A). Inflammasome inhibition and pro-IL-1β reduction appeared within a few hours of IFN-β stimulation (Figure S1A available online) and could not be ascribed to cell death (Figure S1B). Furthermore, by using *Ifnar1*-deficient BMDMs, we ensured that the effects of IFN-β on inflammasome activity and pro-IL-1β were specific to its receptor (Figure 1B). We next asked whether type I IFN could exert similar effects also on bone marrow-derived dendritic cells (BMDCs) and found that caspase-1 activation was inhibited by both IFN-β and IFN-α, whereas the suppressive effect on pro-IL-1β was not observed in this cell type (Figure 1C). Thus, depending on the cell type, type I IFN can regulate the production of the proinflammatory cytokine IL-1β at two levels: by inhibiting inflammasome function and by reducing the pool of intracellular pro-IL-1β.

In order to rule out the possibility that IFN-β-dependent inflammasome suppression was due to interference with LPS priming, NLRP3 inflammasome activity was assayed in cells without prior priming and in cells that were primed with LPS for 4 hr. As shown in Figure 1D, inflammasome-mediated caspase-1 activation was inhibited by IFN-α and -β independently of priming, whereas IFN-γ failed to decrease inflammasome function and intracellular levels of pro-IL-1β under these conditions. Nevertheless, when overnight LPS priming was employed, suppression by type I IFN was most prominent and IFN-γ also displayed inhibitory activity (Figure S1C). In an attempt to determine the mechanisms mediating the observed cross talk between LPS and IFNs, we assessed IFN receptor-proximal signaling and the amounts of signal transducing factors (Figure S1D). No significant differences were observed, suggesting that the diverging responses to type I and II IFNs observed upon different priming regimes are due to downstream integration events of LPS and IFN-β signaling pathways.

Not surprisingly, the secretion of the caspase-1-dependent cytokines IL-1β, IL-18, and IL-1α was strongly diminished when BMDM were pretreated with IFN-β (Figure 1E). In contrast, the amounts of secreted TNF were not significantly altered (Figure S1E), whereas the expression of CD40 and CD86 were even enhanced by IFN-β (Figure S1F). Together, these results show that IFN-β decreases IL-1 and IL-18 production, though it does not affect BMDM activation in a general way.

IFN-β Inhibits NLRP1- and NLRP3-Triggered Inflammasome Activity

To determine whether the suppression exerted by IFN-β specifically affected alum-dependent NLRP3 inflammasome activity, we tested other NLRP3 agonists and found that NLRP3 inflammasome activity after monosodium urate crystals (MSU), asbestos, nigericin, ATP, and *C. albicans* was repressed by IFN-β, similar to alum (Figure 2A).

In order to define whether the effect of IFN-β were confined to NLRP3 or extended to other inflammasome types, we assessed the effects of IFN-β pretreatment on the NLRP1b, IPAF, and AIM2 inflammasomes by activating these inflammasomes with *B. anthracis* lethal toxin (LeTx), *S. typhimurium*, or intracellular delivery of poly(deoxyadenylic-thymidylic) acid (poly(dA:dT)), respectively. Similar to the NLRP3, NLRP1b-dependent inflammasome activity was inhibited by IFN-β (Figure 2B), whereas IPAF-inflammasome and ASC-dependent but NLRP3-independent AIM2-inflammasome were unaffected by IFN-β pretreatment (Figures 2C and 2D). As expected, in all cases mature IL-1β amounts were diminished by IFN-β, reflecting the

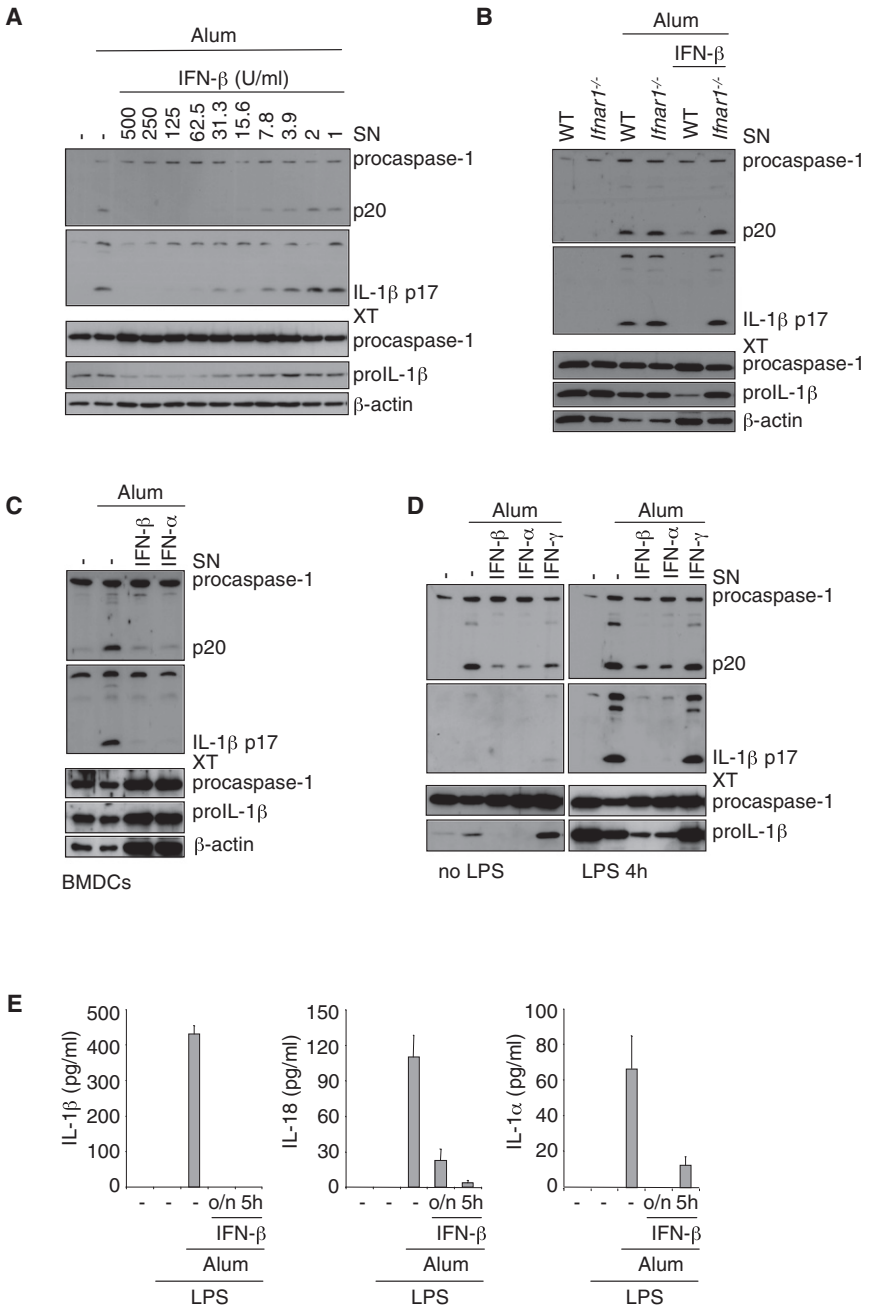

Figure 1. IFN-β Decreases Inflammasome Activity and Pro-IL-1β

(A and B) BMDMs were incubated 12 hr with the indicated doses of IFN-β. Thereafter, LPS was added to prime BMDMs and, 4 hr later, alum stimulation was performed. IL-1β and caspase-1 activation and release were assessed by immunoblot. (B) BMDMs of wild-type (WT) and of *Ifnar1*$^{-/-}$ origin were used.

(C) As for (A), but with BMDCs instead of BMDMs and IFN-β or IFN-α.

(D) BMDMs were incubated overnight with IFN-β, IFN-α, or IFN-γ. LPS was either not added, or added the last 4 hr preceding alum stimulation.

(E) BMDMs were treated with IFN-β overnight for 12 (o/n) or for 5 hr (5h) and primed with LPS for 4 hr. Cells were then stimulated with alum and cytokines measured by ELISA. Data represent mean ± SD of three individual experimental points.

decreased amounts of intracellular pro-IL-1β (Figure 2C and data not shown). Thus, IFN-β specifically inhibits the activity of NLRP1b and NLRP3 inflammasomes.

Type I IFN-Induced IL-10 Controls IL-1β and IL-1α Precursor Levels

A potential role for STAT3 in the suppressive effects downstream of IFNAR was suggested by the inflammatory phenotype of *Stat3* myeloid-specific conditional deleted mice (LysMcre *Stat3*$^{flox/-}$) (Takeda et al., 1999). Though type I IFN-dependent caspase-1 inhibition was unaltered by *Stat3* deletion when compared to control *Stat3*$^{flox/-}$ BMDMs (Figure 3A), the reduction of intracellular pro-IL-1β and pro-IL-1α was much less prominent in *Stat3*-deficient cells (Figure 3A). This suggested that type I IFN induces an inhibitory factor, which is likely to signal via STAT3, that diminishes IL-1β and IL-1α precursor amounts.

Given that the evidence for STAT3 involvement in IFNAR signaling is not compelling and that STAT3 is known to be involved in signaling downstream of IL-10 receptor (IL-10R), we tested the contribution of the anti-inflammatory cytokine IL-10 to the reduction of IL-1 precursor protein. We found that the suppression of LPS-induced pro-IL-1β and pro-IL-1α amounts induced by 5 hr or overnight incubation with IFN-β was strongly abolished in *Il10*$^{-/-}$ BMDMs (Figure 3B; Figure S2). In line with this, exogenous IL-10 decreased the abundance of IL-1β and IL-1α precursor proteins in wild-type (WT) cells (Figure 3C), whereas this was not the case in LysMcre *Stat3*$^{flox/-}$ BMDMs, suggesting a crucial role for STAT3 in the IL-10-mediated reduction of pro-IL-1β and pro-IL-1α amounts. *Ifnar1*$^{-/-}$ and BMDMs lacking the IFN key transcription factor STAT1 (*Stat1*$^{-/-}$) diminished IL-1 precursor amounts in response to IL-10, but failed to do so upon type I IFN (Figure 3C), indicating that IL-10 production is downstream of IFNAR-triggered pathway. Taken together, these results suggest a model in which type I IFN induces secretion of IL-10, which subsequently downregulates pro-IL-1 expresssion through activation of IL-10R and STAT3.

In support of such a mechanism, we found strong IL-10 secretion by WT and conditional LysMcre *Stat3*$^{flox/-}$ BMDMs upon type I IFN plus subsequent LPS exposure, which was not apparent in *Ifnar1*$^{-/-}$ and *Stat1*$^{-/-}$ cells (Figure 3D).

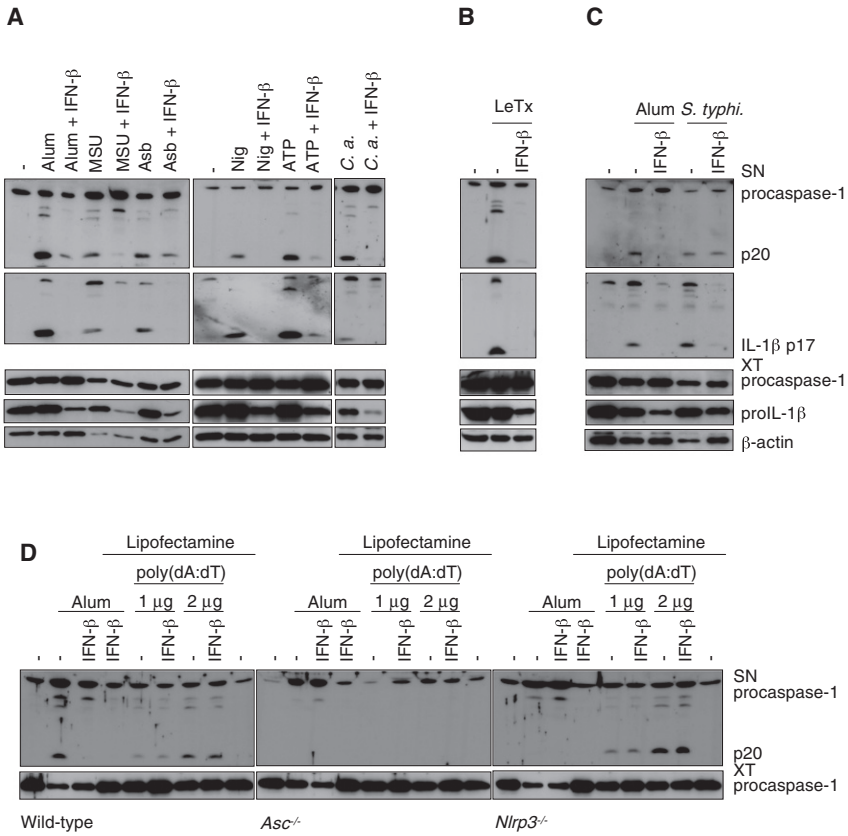

Figure 2. IFN-β Inhibits NLRP3 and NLRP1b Inflammasomes

BMDMs were cultured overnight in the presence or absence of IFN-β. LPS was added to prime the BMDMs during the last 4 hr preceding inflammasome stimulation. Data are representative of at least three individual experiments.

(A–C) Caspase-1 activation and IL-1β release in supernatants after stimulation with alum, MSU, asbestos (Asb), nigericin (Nig), ATP, and *C. albicans* (*C.a.*) (A), after LeTx stimulation (B), or after *S. typhimurium* (*S. typhi.*) infection (C).

(D) Caspase-1 release by BMDMs of WT, *Asc*$^{-/-}$, and *Nlrp3*$^{-/-}$ origin after poly(dA:dT) transfection.

Type I IFN Inhibits NLRP3 Inflammasome Activation in a STAT1-Dependent Manner

Next, we tested whether inflammasome inhibition by type I IFN was mediated via the IFNAR-STAT1 pathway. Indeed in *Stat1*$^{-/-}$ cells, type I IFN could no longer inhibit caspase-1 activation (Figure 4A).

STAT1 can be phosphorylated at residues tyrosine 701 or serine 727. Tyrosine phosphorylation is required for nuclear translocation of STAT1 and transcription factor function (Platanias, 2005). We therefore tested whether type I IFN efficiently suppressed the inflammasome in BMDMs in which STAT1 can be exclusively phosphorylated at the tyrosine residue (in which serine 727 is substituted with an alanine residue (*Stat1*$_{S727A}$)). Our results indicate that serine phosphorylation is dispensable (Figure 4B), suggesting that tyrosine phosphorylation is sufficient for inflammasome inhibition.

Next, we asked whether the inflammasome inhibitory factor was secreted. We tried to rescue type I IFN-dependent inflammasome inhibition in *Ifnar1*$^{-/-}$ BMDMs by coculturing these cells with caspase-1-deficient (*Casp1*$^{-/-}$) BMDMs, which should normally respond to IFN. As shown in Figure 4C, *Casp1*$^{-/-}$ cells were unable to restore inflammasome inhibition in *Ifnar1*$^{-/-}$ cells, suggesting that the inhibitory factor is unlikely to be secreted. Because the known inflammasome components NLRP3, ASC, and caspase-1 also appeared not to be downregulated by type I IFN (Figure 4D), we hypothesized that an intracellular negative regulator of the inflammasome may be induced by STAT1. Several proteins have been suggested to function as caspase-1 or inflammasome inhibitors, including the proteinase inhibitors serpin peptidase inhibitor, clade B, member 9 (Serpinb9, also called SPI-6) and Serpinb2 (also known as PAI-2), caspase-12, pyrin (also called mediterranean fever), and the Bcl family members Bcl-2 and Bcl-XL (also known as BCL2-like 1) (Guarda and So, 2010). We examined whether these candidates were upregulated by type I IFN (by using as a control the IFN-inducible chemokine CXCL10) or whether their deletion affected inflammasome activity (Figures S3A and S3B). However, none of these proteins were significantly induced by type I IFN or were essential for IFN-mediated inhibition of the inflammasome.

Taken together, our results indicate that STAT1 inhibits NLRP3-mediated caspase-1 activation by an as yet undefined mechanism.

Type I IFN Suppresses IL-1-Dependent Inflammatory Cell Recruitment In Vivo

We next asked whether the effects of in vitro IFN treatment on IL-1 production were similar in vivo. We pretreated mice intravenously (i.v.) with polyinosinic-polycytidylic acid (poly(I:C)), a synthetic RNA analog that strongly induces type I IFN production, and subsequently injected them with alum intraperitoneally (i.p.), thus inducing an IL-1-dependent peritonitis that is lost in *Il1r1*$^{-/-}$ mice, as illustrated in Figure S4A. Peritoneal exudate cells (PECs) were collected and cytokine content in the lavages was measured. We found that alum challenge upregulated mature IL-1β secretion in the lavage fluid and that this was prevented by poly(I:C) pretreatment (Figure 5A). We also observed that pro-IL-1β amounts were reduced in PEC extracts from mice pretreated with poly(I:C) (Figure 5B), whereas pro-IL-1α was undetectable (data not shown). All of the aforementioned effects were not observed in *Ifnar1*$^{-/-}$ animals (Figures 5A and 5B), indicating that the effects elicited by poly(I:C) treatment are dependent on type I IFN.

We consequently analyzed alum-induced recruitment of inflammatory cells in control mice or in mice pretreated i.v. with poly(I:C). The number of total PECs recruited upon alum challenge was strongly reduced in mice pretreated with poly(I:C) (Figure 5C). In line with this observation, neutrophil and Ly6C^{+}

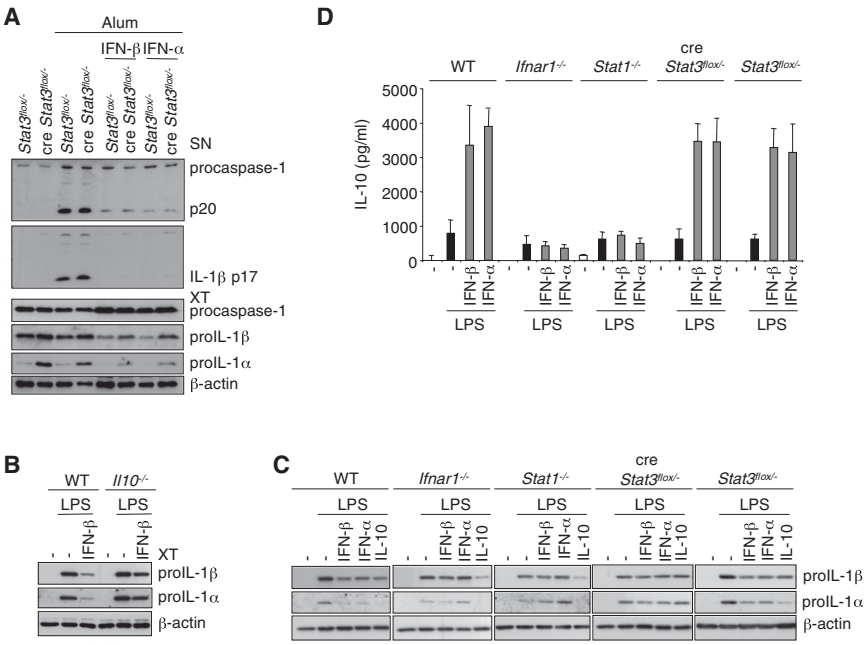

Figure 3. Type I IFN Regulates Pro-IL-1 Levels via IL-10 and STAT3

(A) BMDMs from control (*Stat3*$^{flox/-}$) or LysMcre *Stat3*$^{flox/-}$ (cre *Stat3*$^{flox/-}$) mice were incubated 12 hr with IFN-β or IFN-α. Thereafter, LPS was added to prime the BMDMs and, 4 hr later, alum stimulation was performed. Caspase-1 activation and IL-1β release are shown in supernatants, procaspase-1, pro-IL-1β, or pro-IL-1α levels in cell lysates.

(B) BMDMs from WT or *Il10*$^{-/-}$ mice were incubated 5 hr with IFN-β, followed by 4 hr LPS treatment. Pro-IL-1β and pro-IL-1α levels were assessed in cell lysates.

(C and D) BMDMs from WT, *Ifnar1*$^{-/-}$, *Stat1*$^{-/-}$, LysMcre *Stat3*$^{flox/-}$, or control (*Stat3*$^{flox/-}$) mice were incubated 5 hr with IFN-β, IFN-α (C and D), or IL-10 (C), followed by 4 hr LPS treatment. Pro-IL-1β and pro-IL-1α levels in cell lysates were measured by immunoblot (C), IL-10 levels by ELISA (D). Data represent mean ± SD of three individual experimental points (D).

monocyte recruitment was significantly blocked by poly(I:C) pretreatment (Figures 5D and 5E). In order to exclude the probability that the observed reduction was due to a general defect induced by poly(I:C) on migratory cells, zymosan, which is known to induce a peritonitis independently of IL-1, was used in parallel (Figures 5C–5E; Dostert et al., 2009; Martinon et al., 2006). In this case, PECs, neutrophils, and (to a lesser extent) Ly6C^{+} monocytes were still recruited to the peritoneum despite the poly(I:C) pretreatment, further demonstrating that poly(I:C) suppresses alum-induced peritonitis by blocking the generation of IL-1.

Again, the effects of poly(I:C) were specific to type I IFN, as shown by the fact that poly(I:C) pretreatment did not alter the recruitment of total PECs and neutrophils and affected Ly6C^{+} monocyte influx only in a minor proportion in *Ifnar1*$^{-/-}$ mice (Figures 5F–5H).

It was reported that poly(I:C) itself can induce IL-1β through activation of the NLRP3 inflammasome (Allen et al., 2009; Kanneganti et al., 2006). Although we can confirm that poly(I:C) primes cells for pro-IL-1β synthesis, particularly in vitro, we found no evidence for direct inflammasome activation by

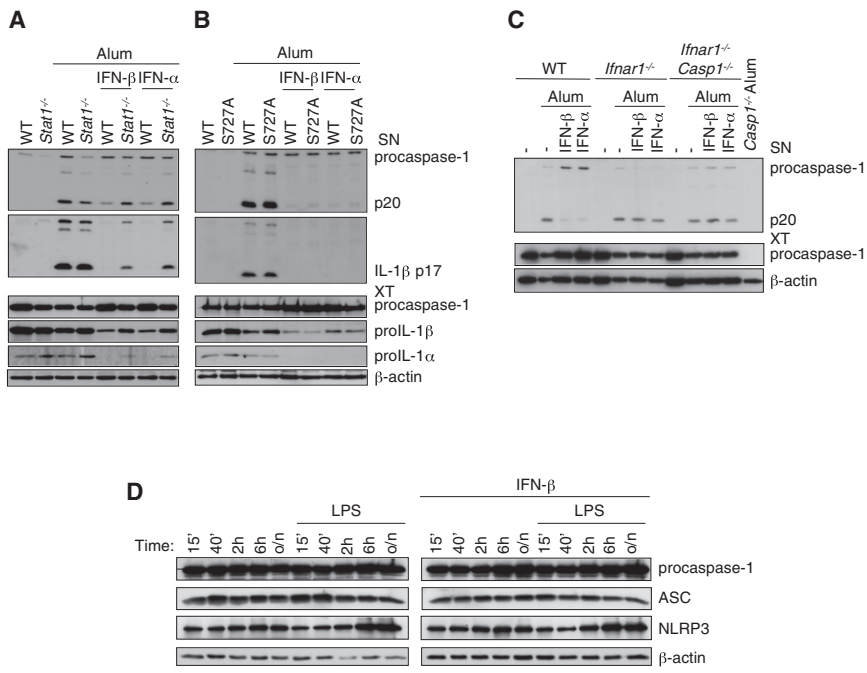

Figure 4. Inflammasome Inhibition by Type I IFN Is STAT1 Dependent

(A and B) C57BL/6 (WT), *Stat1*$^{-/-}$ (A), and *Stat1*$_{S727A}$ knockin (S727A) (B) BMDMs were incubated 12 hr with IFN-β or IFN-α. Thereafter, LPS was added to prime the BMDMs and, 4 hr later, alum stimulation was performed. Caspase-1 activation and IL-1β release are shown in supernatants, procaspase-1, pro-IL-1β, and pro-IL-1α levels in cell lysates.

(C) BMDMs from C57BL/6 (WT), *Ifnar1*$^{-/-}$, or *Caspase1*$^{-/-}$ (*Casp1*$^{-/-}$) were cultured alone or cocultured as indicated. Cells were incubated 12 hr with IFN-β or IFN-α, followed by 4 hr LPS and alum stimulation. Caspase-1 activation was assessed by immunoblot in culture supernatants.

(D) BMDMs were stimulated for the indicated times with LPS, IFN-β , or a combination of the two. Expression of inflammasome components was assessed by immunoblot in cell lysates.

Data are representative of two to four individual experiments.

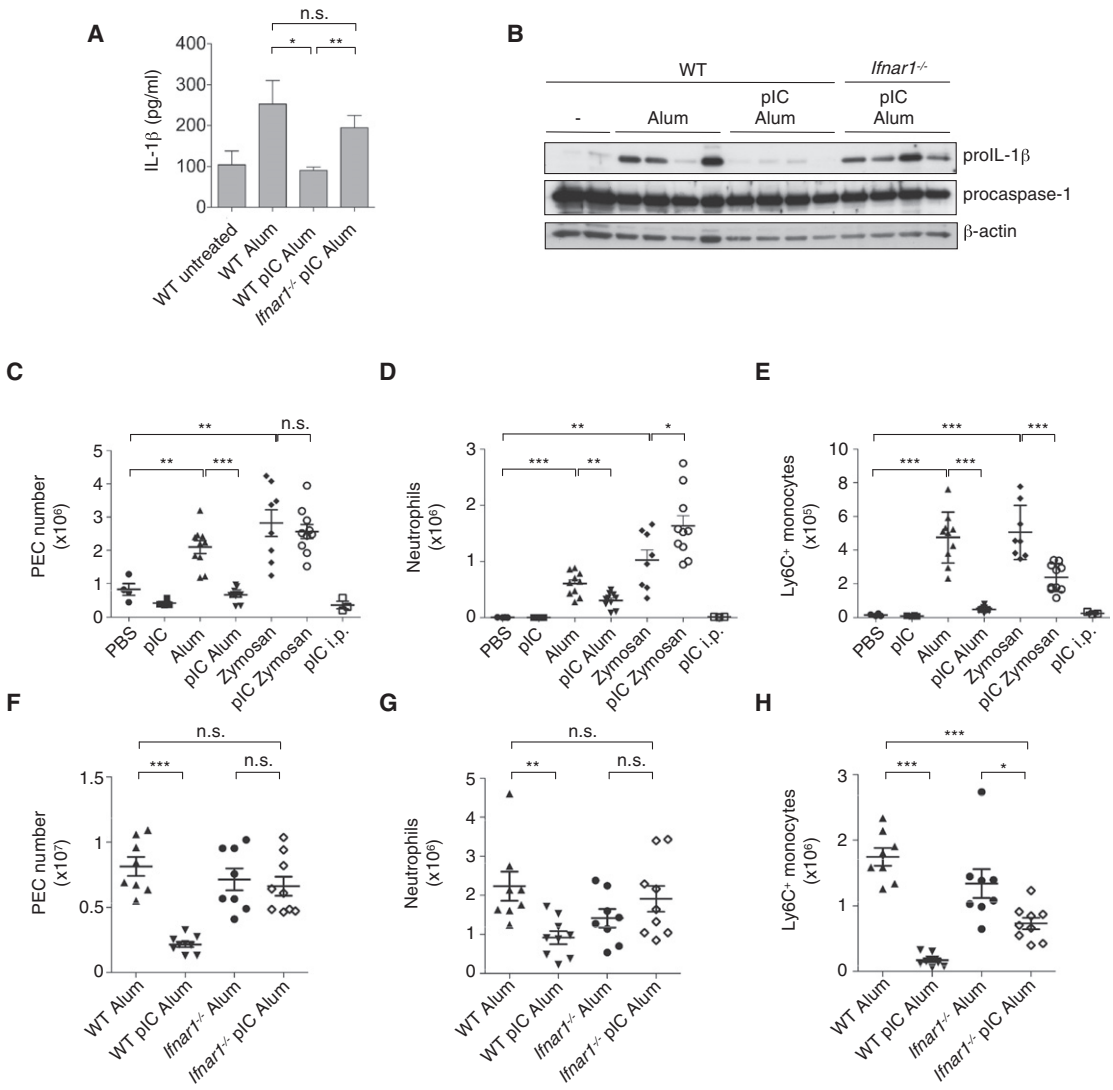

Figure 5. Type I IFN Decreases the Inflammatory Response to Alum

C57BL/6 or *Ifnar1*$^{-/-}$ mice were injected with poly(I:C) (pIC) i.v. or left untreated as a control. 5 hr later, mice were challenged with alum, zymosan, or poly(I:C) (pIC i.p.) i.p.

(A and B) 2 hr after alum injection, peritoneal cavities were lavaged. IL-1β content in the lavage fluid was measured by ELISA (A), while PECs recovered were lysed and analyzed for their expression of pro-IL-1β by immunoblot (B). Values are the mean ± SEM of five to eight mice per group, pooled from two independent experiments (A), while in (B) individual mice are represented in each lane.

(C–E) 12–14 hr after alum or zymosan injection, mice were sacrificed and peritoneal lavages performed. Absolute numbers of PECs, neutrophils, or Ly6C^{+} monocytes recruited to the peritoneum are depicted.

(F–H) 12–14 hr after alum injection, C57BL/6 or *Ifnar1*$^{-/-}$ mice were sacrificed and peritoneal lavages performed. Absolute numbers of PECs, neutrophils, or Ly6C^{+} monocytes recruited to the peritoneum are depicted.

(C–H) Data represent mean ± SEM of the pool of two independent experiments, and results for individual mice are illustrated.

poly(I:C) in vitro (Figures S4B and S4C). We also saw no evidence for poly(I:C)-dependent inflammasome activation in vivo (Figure 5D), because i.p. injection of poly(I:C) did not trigger neutrophil influx, a hallmark of IL-1 production (Chen et al., 2006).

Type I IFN Increases Susceptibility to *C. albicans* Infection

Treatment of mice with poly(I:C) impairs their survival to *C. albicans* infection (Jensen et al., 1992; Worthington and Hasenclever, 1972). Given the importance of IL-1 in the control of this infection (Figure S5A; Bellocchio et al., 2004), we wondered whether under those circumstances, poly(I:C)-induced type I IFN might decrease IL-1, thus explaining increased susceptibility to *C. albicans*. We compared survival after *C. albicans* challenge of naive or poly(I:C)-pretreated WT mice and *Ifnar1*$^{-/-}$ mice. Poly(I:C)-primed WT mice showed dramatically increased susceptibility to *C. albicans* infection as compared to unprimed mice (Figure 6A), whereas poly(I:C)-primed *Ifnar1*$^{-/-}$ mice survived *C. albicans* challenge similar to unprimed animals (Figure 6B). The premature death of WT poly(I:C)-treated animals was found

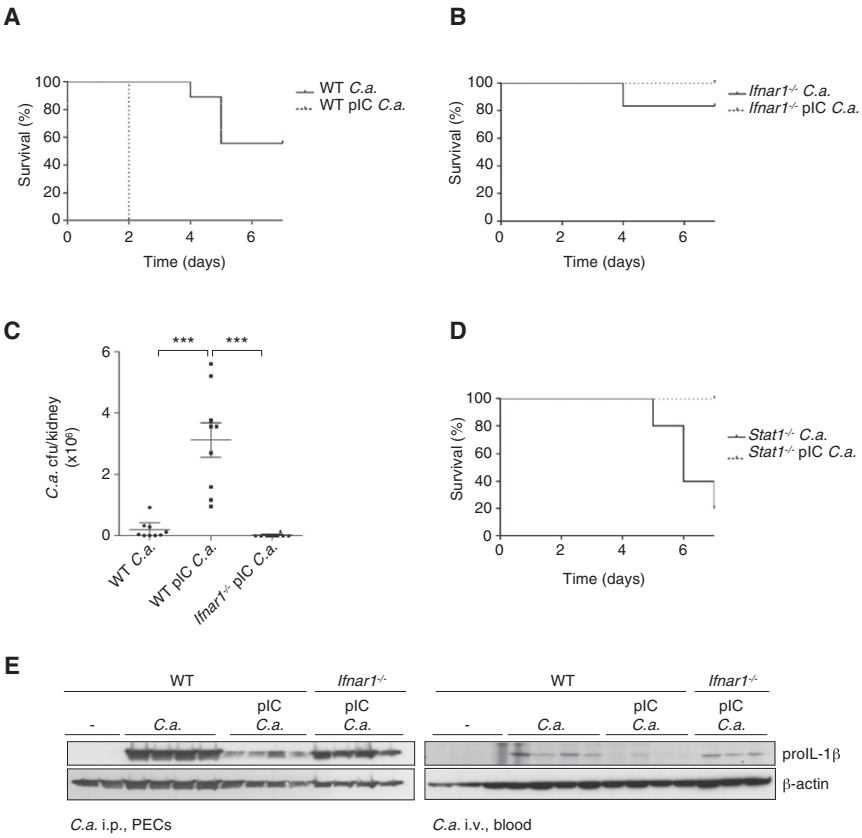

Figure 6. Type I IFN Worsens Susceptibility to *C. albicans* Infection

(A–D) WT, *Ifnar1*$^{-/-}$, or *Stat1*$^{-/-}$ mice were treated or not with poly(I:C) (pIC) i.v. and 5 hr later, mice were infected i.v. with *C. albicans* (*C.a.*). On day 1, poly(I:C)-treated mice were injected a second time with poly(I:C).

(A, B, D) Survival of the different cohorts of mice was monitored for 7 days postinfection. Data are representative of at least two independent experiments (per condition, n = 9–10 for WT, n = 4–6 for *Ifnar1*$^{-/-}$ or *Stat1*$^{-/-}$ mice).

(C) *C. albicans* load was assessed in the kidneys of 2 day infected mice by counting *C. albicans* cfu/kidney in the indicated groups. Cfu per kidney are represented as mean ± SEM of the pool of two experiments (9–10 mice per group).

(E) WT or *Ifnar1*$^{-/-}$ mice were treated or not with poly(I:C) i.v. and 5 hr later, mice were infected i.p. with 10^6 or i.v. with 10^7 *C. albicans* fungal cells. 3 hr after i.p. injection and 5 hr after i.v. injection, PECs or blood were harvested, respectively. Intracellular content of pro-IL-1β was then assessed by immunoblot.

to be due to a defective control of *C. albicans*, as indicated by the fact that kidneys of these animals contained significantly more colony forming units (CFU) than the kidneys of unprimed WT mice and the kidneys of poly(I:C)-treated *Ifnar1*$^{-/-}$ animals (Figure 6C). We also tested the outcome of poly(I:C) priming on *C. albicans* infection in *Stat1*$^{-/-}$ mice (Figure 6D). As expected, *Stat1*$^{-/-}$ mice resisted the detrimental effects of poly(I:C) priming on candidiasis progression. Intriguingly, we noticed that poly (I:C)-primed *Stat1*$^{-/-}$ mice and, to a lesser extent, poly(I:C)-primed *Ifnar1*$^{-/-}$ animals showed a tendency to slightly better survive *C. albicans* infection compared to their unprimed counterparts (Figures 6B and 6D). We also assessed the role of IFN-γ in STAT1-mediated *C. albicans* susceptibility and found, as predicted from our in vitro data, that type II IFN is not playing a dominant role (Figure S5B).

We then verified whether poly(I:C)-induced type I IFN was indeed reducing the IL-1 response to *C. albicans* in vivo. We challenged poly(I:C)-primed or -unprimed WT and *Ifnar1*$^{-/-}$ animals with *C. albicans* i.p. or i.v. and then analyzed the levels of pro-IL-1β in PECs and blood, respectively. As shown in Figure 6E, poly(I:C)-induced type I IFN clearly decreased the ability of the mice to produce pro-IL-1β upon *C. albicans* challenge.

IFN-β Suppresses IL-1β Production in Human Primary Monocytes

To investigate whether type I IFN exerts the same anti-inflammatory effects in human cells, primary monocytes were isolated from blood of healthy donors (HDs) and cultured overnight with IFN-β, primed with LPS, and then stimulated with alum. In line with findings from mice, incubation with IFN-β effectively diminished alum-induced IL-1β secretion and caspase-1 cleavage (Figures 7A and 7B). As shown in Figure 7C, even at low concentrations IFN-β significantly suppressed IL-1β production. Similar to what was observed in mouse BMDMs, a striking decrease in pro-IL-1β accompanied by IL-10 induction was noted (Figure 7B; Figure S6A). Thus, type I IFN plays a crucial role in the negative regulation of both caspase-1 activity and pro-IL-1β production in human primary monocytes.

IFN-β is currently used in the management of several diseases including MS. We therefore asked whether IFN-β treatment in RR-MS patients similarly suppresses IL-1β production. First, we confirmed that the recombinant IFN-β preparations administered to the patients (IFN-β-1a, Rebif, produced in mammalian cells, and IFN-β-1b Betaferon, produced in bacteria) had the same in vitro effects on IL-1β production as the IFN-β used for research purposes (Figure S6B). Finally, monocytes isolated from blood of MS patients on IFN-β therapy were challenged ex vivo with alum in the presence or the absence of LPS priming or left untreated (Figure 7D). IL-1β production by monocytes derived from both Rebif- and Betaferon-treated patients released significantly less IL-1β than monocytes derived from HDs. Taken together, these results suggest that a possible mode of action for the success of IFN-β treatment for MS might indeed rely on suppressing IL-1-mediated inflammation.

DISCUSSION

In addition to its antiviral effects, type I IFN is acknowledged as an immunomodulatory cytokine, though the underlying mechanisms are poorly understood. Our work suggests that

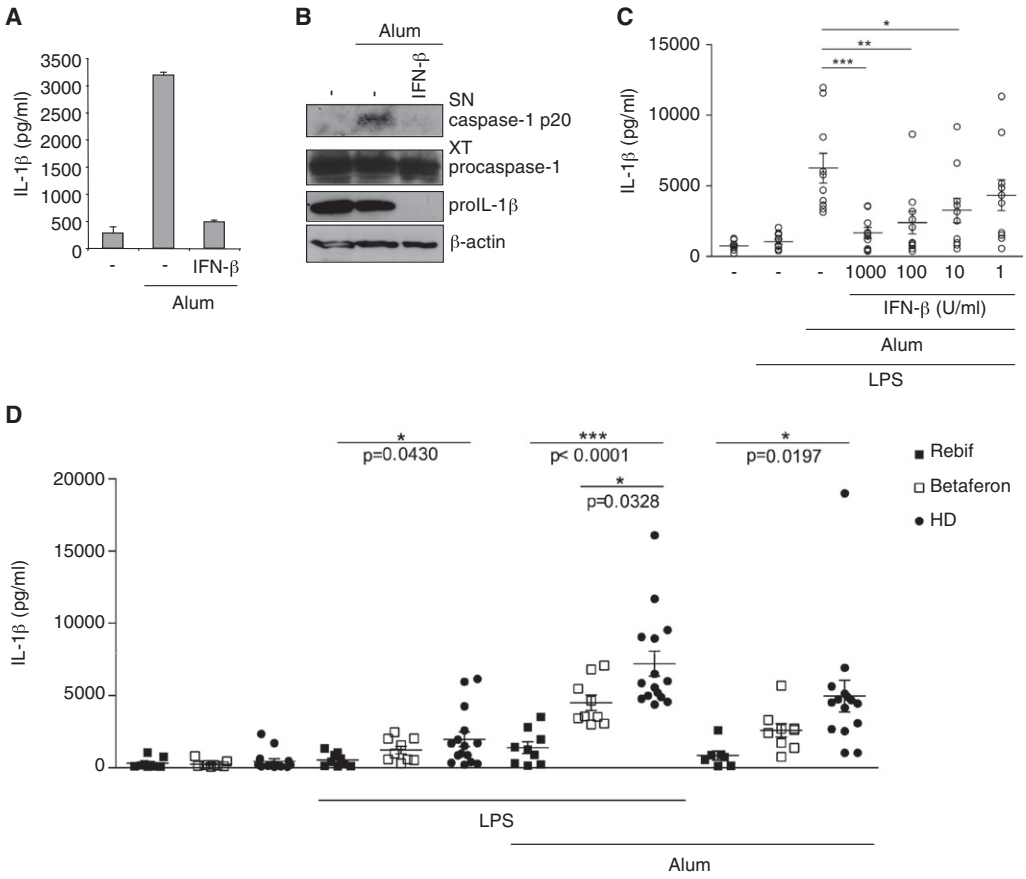

Figure 7. IFN-β Suppresses IL-1β Production by Human Primary Monocytes

(A–C) Human primary monocytes were cultured overnight in the presence of 1000 U/ml (A, B) or the indicated doses of human IFN-β (C). LPS was added to prime the monocytes for 3 hr, followed by stimulation with alum. IL-1β release was measured by ELISA and data represent mean ± SD of 3 experimental replicates (A) or mean ± SEM of 10 individual donors (C). Caspase-1 activation in the supernatants after stimulation with alum and pro-IL-1β levels in cell lysates are shown in (B). (D) Monocytes from RR-MS patients treated with Rebif or Betaferon, and in parallel, from age- and gender-matched HDs were primed with 3 hr LPS exposure or left unprimed. Then, cells were stimulated with alum. IL-1β release was measured by ELISA and data represent mean ± SEM of 9 Rebif-treated RR-MS patients, 9 Betaferon-treated RR-MS patients, and 15 untreated healthy donors.

the anti-inflammatory effects exerted by type I IFN may be due at least partially to its ability to control IL-1 production. IL-1α, which does not require processing by caspase-1, is reduced in BMDMs upon incubation with type I IFN, whereas secretion of active IL-1β is abolished by two distinct means: through the reduction of pro-IL-1β protein and via suppression of NLRP1b and NLRP3 inflammasome-dependent caspase-1 activation. Such inflammasome inhibition by IFN also provides a mechanism for the observed interferon-dependent suppression of IL-18 maturation, as shown by the fact that IL-18 maturation also depends on inflammasome activity.

The predominant mechanism leading to type I IFN-dependent suppression of pro-IL-1β and pro-IL-1α is based on the STAT1-mediated synergistic action of type I IFN and LPS to induce IL-10. IL-10, in turn, regulates pro-IL-1β and pro-IL-1α amounts in a STAT3-dependent manner. In agreement with a previous report (Hu et al., 2006), the ability to induce IL-10 is specific to type I IFN, thus nicely supporting our observation that IFN-γ does not significantly decrease the levels of pro-IL-1β and pro-IL-1α. The mechanism by which IL-10 exerts its anti-inflammatory effects is still the object of intense research, but the reduction of IL-1 precursor levels may represent one important pathway.

STAT1 is crucial for the inhibition of NLRP3 inflammasome activity by type I IFNs. We found that phosphorylation at tyrosine 701 was sufficient for the suppression of NLRP3 inflammasome activity, whereas the serine 727 modification was dispensable. Tyrosine phosphorylation is required and sufficient for STAT1 nuclear translocation and DNA binding to target promotors, whereas modification of serine 727 appears to enhance STAT1 transactivator function. This suggests that transcriptional induction of a target gene was required for the inflammasome-suppressing activity of type I IFN. Our results also indicate that the inhibitory pathway is likely to be cell intrinsic, but future studies will be needed to further characterize this pathway.

IL-1β has been reported to play a role in controlling viral infections such as influenza. Moreover, viral RNA and poly(I:C) were reported to induce release of IL-1β through activation of the NLRP3 inflammasome (Allen et al., 2009; Kanneganti et al., 2006). Interestingly, we observed an increase in intracellular pro-IL-1β upon poly(I:C) exposure, in particular in vitro. However,

we could detect neither activation of caspase-1 nor release of mature IL-1β under these circumstances. In vivo, poly(I:C) triggered strong induction of type I IFN that efficiently prevented further pro-IL-1β induction by exogenous inflammasome agonists. Hence, depending on the type of infection, the balance between the induction of type I IFN and pro-IL-1β could indeed dictate the final level of mature IL-1β.

The capacity of type I IFNs to suppress inflammasome activity and IL-1 production is relevant to the phenomenon of superinfections. It is well established that although infections with viruses such as influenza are very common, mortalities purely attributable to the primary viral infection are relatively rare. Many influenza-related deaths are caused by secondary bacterial infections, which present a unique clinical challenge resulting from the emergence of antibiotic resistance and increased severity of infection. Influenza infections impair innate immune function and several mechanisms for the increased susceptibility to secondary bacterial infections have been proposed, some of which are dependent on type I IFNs (Shahangian et al., 2009). Our data suggest that the ability of type I IFN to suppress inflammasome activity and IL-1 secretion may contribute to the increased risk of infection after viral exposure. In line with this, we showed that poly(I:C)-induced type I IFN rendered WT mice as susceptible to *C. albicans* infection as *Il1r1*$^{-/-}$ mice (Bellocchio et al., 2004; Kullberg et al., 1990; Van't Wout et al., 1988; Vonk et al., 2006). To further corroborate our hypothesis, we showed that poly(I:C)-induced type I IFN suppressed an effective IL-1 response to *C. albicans* infection. In an analogous manner, Medzhitov's laboratory delineated a mechanism by which influenza virus leads to suppression of the host immune response and to increased susceptibility to secondary bacterial infection through glucocorticoid induction (Jamieson et al., 2010). Interestingly, IL-1β is inhibited by glucocorticoid hormones in vivo and in vitro (Fantuzzi and Ghezzi, 1993).

The contributions of IL-1 and IL-18 to the development of inflammatory and autoimmune manifestations are well described (Chae et al., 2009; Furlan et al., 1999a, 1999b; Kantarci et al., 2002). These include MS, where interleukin-1β and interleukin-1 receptor antagonist gene polymorphisms were found to be associated with disease severity (Kantarci et al., 2002). Although more experimental evidence is required, it is tempting to speculate that the successful treatment of MS with IFN is mediated, at least in part, by its ability to suppress the IL-1-inflammasome axis. Such a notion is supported by our observation that inflammasome activity is suppressed in monocytes from patients under IFN therapy. Our data retrospectively shed light on some aspects of the widespread use of IFN in the treatment of autoimmune and/or inflammatory diseases and suggest that inflammasome inhibitors may complement current treatment regimes.

EXPERIMENTAL PROCEDURES

Mice

Mice were treated in accordance with the Swiss Federal Veterinary Office guidelines.

In Vitro Stimulation Experiments

BMDMs and BMDCs were differentiated as previously described (Guarda et al., 2009). 5 × 10^4 differentiated BMDMs or BMDCs were incubated for 12 hr or the indicated times in the presence of 500 U/ml IFN-β, 500 U/ml IFN-α11 (both from PBL Interferon Source), 20 ng/ml IFN-γ (Calbiochem), or 20 ng/ml IL-10 (Peprotech) unless otherwise specified. According to what was indicated, cells were primed with 10 ng/ml ultrapure LPS (Invivogen) either for 12 hr (at the same time as IFN treatment), for the 4–6 hr preceding inflammasome stimulations, or left unprimed. Then, stimulations were carried out. ATP (500 μM), nigericin (0.4 μM), and MSU crystals (300 μg/ml) were from Sigma. Asbestos (300 μg/ml) was from SPI-CHEM and alum (300 μg/ml) from Pierce Biochemicals (Imject-alum). ATP stimulations were performed for 45 min, other stimulations for 150 min (unless otherwise indicated). *C. albicans* was put on BMDMs at a multiplicity of infection of 1 for 150 min. *B. anthracis* LeTx stimulation and *S. typhimurium* infection were carried out as previously described (Guarda et al., 2009). For the stimulation of the AIM-2 inflammasome, poly(dA:dT) (purchased from Amersham) was admixed at the indicated concentrations to Lipofectamine 2000 (from Invitrogen) according to manufacturer's instructions and cells were stimulated for 6 hr.

Isolation of Human Primary Monocytes

We obtained buffy coats from the Lausanne Blood Transfusion Center. Additionally, healthy volunteers and RR-MS patients on Rebif or Betaferon treatment (receiving their last IFN-β injection at the same day or up to 3 days prior to blood collection) donated 40 ml of blood after informed consent. Blood draw for this study was accepted by our institution's ethical commission and all subjects gave their written consent according to review board guidelines.

Stimulation of Human Primary Monocytes

Monocytes from RR-MS patients or healthy donors were plated at 150,000 cells/well and left untreated or primed with 1 ng/ml LPS (Invivogen) for 3 hr. Unprimed or primed monocytes were subsequently stimulated for 6 hr with 500 μg/ml alum (Pierce). For in vitro IFN-β treatment, CD14$^+$ monocytes were incubated with the indicated amounts of IFN-β (Peprotech) for 12 hr followed by 3 hr LPS priming and 6 hr alum stimulation. To test the production of IL-10 upon IFN-β exposure, CD14$^+$ monocytes were incubated in the presence of IFN-β for 12 hr and then stimulated with LPS for 4 hr or left unstimulated.

In Vivo Peritonitis and *Candida albicans* Infection Experiments

For peritonitis, mice were injected i.v., unless otherwise indicated, with 200 μg poly(I:C) (Invivogen) followed by a second i.p. injection of alum 5 hr later. For the analysis of PECs, 350 μg alum (Pierce) or 350 μg zymosan (Invivogen) as control were injected. 12–14 hr after alum injection, mice were sacrificed and peritoneal cavities were washed with 6 ml PBS. PECs were analyzed by FACS. For the analysis of IL-1β in the peritoneal cavity, 5 hr after i.v. injection of 200 μg poly(I:C), mice were injected i.p. with 700 μg alum. Lavages and PECs were harvested 2 hr later, and peritoneal fluids were concentrated for ELISA analysis with Amicon Ultra 10K from Millipore.

C. albicans was cultured on Chromagar Candida plates (BD Bioscience). For *C. albicans* infections, mice were injected i.v., with 200 μg poly(I:C), followed by a second i.v. injection of 2.5 × 10^5 fungal cells 5 hr later. The day after, mice treated with poly(I:C) were injected again i.v. with 100 μg poly(I:C). For analysis of *C. albicans* load, mice were sacrificed 48 hr after infection, and homogenized kidneys were plated on Chromagar Candida plates to determine colony forming units. For survival assay, mice were monitored with a scoresheet, in accordance with local guidelines for animal experimentation.

Statistical Analysis

Statistical differences were calculated with an unpaired Student's t test, two-tailed (GraphPad Prism version 5.0). Differences were considered significant when $p \leq 0.05$ (*), very significant when $p \leq 0.01$ (**), and extremely significant when $p \leq 0.001$ (***).

SUPPLEMENTAL INFORMATION

Supplemental Information includes Supplemental Experimental Procedures and six figures and can be found with this article online at doi:10.1016/j.immuni.2011.02.006.

ACKNOWLEDGMENTS

We acknowledge patients and healthy volunteers for their contribution to this study by donating blood. We thank M. Aguet, ISREC (Lausanne), H. Acha-Orbea, UNIL (Lausanne), A. Suhrbier, Queensland Institute of Medical Research (Brisbane), and P. Ashton-Rickardt, Imperial College London (London) for knockout mice; M. Winter (University of Duesseldorf), R. Castillo, and O. Gross for technical help; and K. Schroder and C. Thomas for critical reading of the manuscript. This work was in part supported by the Swiss National Science Foundation and by the Institute for Arthritis Research. M.B. and P.R. are supported by the Swiss National Science foundation and P.R. also by the NCCR Molecular Oncology.

Received: July 10, 2010
Revised: October 22, 2010
Accepted: December 2, 2010
Published online: February 24, 2011

REFERENCES

Allen, I.C., Scull, M.A., Moore, C.B., Holl, E.K., McElvania-TeKippe, E., Taxman, D.J., Guthrie, E.H., Pickles, R.J., and Ting, J.P. (2009). The NLRP3 inflammasome mediates in vivo innate immunity to influenza A virus through recognition of viral RNA. Immunity *30*, 556–565.

Barkhof, F., Polman, C.H., Radue, E.W., Kappos, L., Freedman, M.S., Edan, G., Hartung, H.P., Miller, D.H., Montalbán, X., Poppe, P., et al. (2007). Magnetic resonance imaging effects of interferon beta-1b in the BENEFIT study: Integrated 2-year results. Arch. Neurol. *64*, 1292–1298.

Bellocchio, S., Montagnoli, C., Bozza, S., Gaziano, R., Rossi, G., Mambula, S.S., Vecchi, A., Mantovani, A., Levitz, S.M., and Romani, L. (2004). The contribution of the Toll-like/IL-1 receptor superfamily to innate and adaptive immunity to fungal pathogens in vivo. J. Immunol. *172*, 3059–3069.

Billiau, A. (2006). Anti-inflammatory properties of Type I interferons. Antiviral Res. *71*, 108–116.

Chae, J.J., Aksentijevich, I., and Kastner, D.L. (2009). Advances in the understanding of familial Mediterranean fever and possibilities for targeted therapy. Br. J. Haematol. *146*, 467–478.

Chen, C.J., Shi, Y., Hearn, A., Fitzgerald, K., Golenbock, D., Reed, G., Akira, S., and Rock, K.L. (2006). MyD88-dependent IL-1 receptor signaling is essential for gouty inflammation stimulated by monosodium urate crystals. J. Clin. Invest. *116*, 2262–2271.

Coclet-Ninin, J., Dayer, J.M., and Burger, D. (1997). Interferon-beta not only inhibits interleukin-1beta and tumor necrosis factor-alpha but stimulates interleukin-1 receptor antagonist production in human peripheral blood mononuclear cells. Eur. Cytokine Netw. *8*, 345–349.

Comi, G., Filippi, M., Barkhof, F., Durelli, L., Edan, G., Fernández, O., Hartung, H., Seeldrayers, P., Sørensen, P.S., Rovaris, M., et al; Early Treatment of Multiple Sclerosis Study Group. (2001). Effect of early interferon treatment on conversion to definite multiple sclerosis: A randomised study. Lancet *357*, 1576–1582.

Decker, T., Müller, M., and Stockinger, S. (2005). The yin and yang of type I interferon activity in bacterial infection. Nat. Rev. Immunol. *5*, 675–687.

Dostert, C., Guarda, G., Romero, J.F., Menu, P., Gross, O., Tardivel, A., Suva, M.L., Stehle, J.C., Kopf, M., Stamenkovic, I., et al. (2009). Malarial hemozoin is a Nalp3 inflammasome activating danger signal. PLoS ONE *4*, e6510.

Fantuzzi, G., and Ghezzi, P. (1993). Glucocorticoids as cytokine inhibitors: Role in neuroendocrine control and therapy of inflammatory diseases. Mediators Inflamm. *2*, 263–270.

Furlan, R., Filippi, M., Bergami, A., Rocca, M.A., Martinelli, V., Poliani, P.L., Grimaldi, L.M., Desina, G., Comi, G., and Martino, G. (1999a). Peripheral levels of caspase-1 mRNA correlate with disease activity in patients with multiple sclerosis; a preliminary study. J. Neurol. Neurosurg. Psychiatry *67*, 785–788.

Furlan, R., Martino, G., Galbiati, F., Poliani, P.L., Smiroldo, S., Bergami, A., Desina, G., Comi, G., Flavell, R., Su, M.S., and Adorini, L. (1999b). Caspase-1 regulates the inflammatory process leading to autoimmune demyelination. J. Immunol. *163*, 2403–2409.

Giovannoni, G., and Miller, D.H. (1999). Multiple sclerosis and its treatment. J. R. Coll. Physicians Lond. *33*, 315–322.

Gross, O., Poeck, H., Bscheider, M., Dostert, C., Hannesschläger, N., Endres, S., Hartmann, G., Tardivel, A., Schweighoffer, E., Tybulewicz, V., et al. (2009). Syk kinase signalling couples to the Nlrp3 inflammasome for anti-fungal host defence. Nature *459*, 433–436.

Guarda, G., and So, A. (2010). Regulation of inflammasome activity. Immunology *130*, 329–336.

Guarda, G., Dostert, C., Staehli, F., Cabalzar, K., Castillo, R., Tardivel, A., Schneider, P., and Tschopp, J. (2009). T cells dampen innate immune responses through inhibition of NLRP1 and NLRP3 inflammasomes. Nature *460*, 269–273.

Hu, X., Paik, P.K., Chen, J., Yarilina, A., Kockeritz, L., Lu, T.T., Woodgett, J.R., and Ivashkiv, L.B. (2006). IFN-gamma suppresses IL-10 production and synergizes with TLR2 by regulating GSK3 and CREB/AP-1 proteins. Immunity *24*, 563–574.

Huang, Y., Blatt, L.M., and Taylor, M.W. (1995). Type 1 interferon as an antiinflammatory agent: Inhibition of lipopolysaccharide-induced interleukin-1 beta and induction of interleukin-1 receptor antagonist. J. Interferon Cytokine Res. *15*, 317–321.

Jamieson, A.M., Yu, S., Annicelli, C.H., and Medzhitov, R. (2010). Influenza virus-induced glucocorticoids compromise innate host defense against a secondary bacterial infection. Cell Host Microbe *7*, 103–114.

Jensen, J., Vazquez-Torres, A., and Balish, E. (1992). Poly(I.C)-induced interferons enhance susceptibility of SCID mice to systemic candidiasis. Infect. Immun. *60*, 4549–4557.

Kanneganti, T.D., Body-Malapel, M., Amer, A., Park, J.H., Whitfield, J., Franchi, L., Taraporewala, Z.F., Miller, D., Patton, J.T., Inohara, N., and Núñez, G. (2006). Critical role for Cryopyrin/Nalp3 in activation of caspase-1 in response to viral infection and double-stranded RNA. J. Biol. Chem. *281*, 36560–36568.

Kantarci, O.H., de Andrade, M., and Weinshenker, B.G. (2002). Identifying disease modifying genes in multiple sclerosis. J. Neuroimmunol. *123*, 144–159.

Kötter, I., Günaydin, I., Zierhut, M., and Stübiger, N. (2004). The use of interferon alpha in Behçet disease: Review of the literature. Semin. Arthritis Rheum. *33*, 320–335.

Kullberg, B.J., van 't Wout, J.W., and van Furth, R. (1990). Role of granulocytes in increased host resistance to *Candida albicans* induced by recombinant interleukin-1. Infect. Immun. *58*, 3319–3324.

Lara-Tejero, M., Sutterwala, F.S., Ogura, Y., Grant, E.P., Bertin, J., Coyle, A.J., Flavell, R.A., and Galán, J.E. (2006). Role of the caspase-1 inflammasome in *Salmonella typhimurium* pathogenesis. J. Exp. Med. *203*, 1407–1412.

Martinon, F., Burns, K., and Tschopp, J. (2002). The inflammasome: a molecular platform triggering activation of inflammatory caspases and processing of proIL-beta. Mol. Cell *10*, 417–426.

Martinon, F., Pétrilli, V., Mayor, A., Tardivel, A., and Tschopp, J. (2006). Gout-associated uric acid crystals activate the NALP3 inflammasome. Nature *440*, 237–241.

Martinon, F., Mayor, A., and Tschopp, J. (2009). The inflammasomes: Guardians of the body. Annu. Rev. Immunol. *27*, 229–265.

Masters, S.L., Mielke, L.A., Cornish, A.L., Sutton, C.E., O'Donnell, J., Cengia, L.H., Roberts, A.W., Wicks, I.P., Mills, K.H., and Croker, B.A. (2010). Regulation of interleukin-1beta by interferon-gamma is species specific, limited by suppressor of cytokine signalling 1 and influences interleukin-17 production. EMBO Rep. *11*, 640–646.

McDermott, M.F., and Tschopp, J. (2007). From inflammasomes to fevers, crystals and hypertension: How basic research explains inflammatory diseases. Trends Mol. Med. *13*, 381–388.

Meylan, E., Tschopp, J., and Karin, M. (2006). Intracellular pattern recognition receptors in the host response. Nature *442*, 39–44.

Mosley, B., Urdal, D.L., Prickett, K.S., Larsen, A., Cosman, D., Conlon, P.J., Gillis, S., and Dower, S.K. (1987). The interleukin-1 receptor binds the human interleukin-1 alpha precursor but not the interleukin-1 beta precursor. J. Biol. Chem. *262*, 2941–2944.

Platanias, L.C. (2005). Mechanisms of type-I- and type-II-interferon-mediated signalling. Nat. Rev. Immunol. *5*, 375–386.

Schroder, K., Muruve, D.A., and Tschopp, J. (2009). Innate immunity: Cytoplasmic DNA sensing by the AIM2 inflammasome. Curr. Biol. *19*, R262–R265.

Shahangian, A., Chow, E.K., Tian, X., Kang, J.R., Ghaffari, A., Liu, S.Y., Belperio, J.A., Cheng, G., and Deng, J.C. (2009). Type I IFNs mediate development of postinfluenza bacterial pneumonia in mice. J. Clin. Invest. *119*, 1910–1920.

Stetson, D.B., and Medzhitov, R. (2006). Type I interferons in host defense. Immunity *25*, 373–381.

Takeda, K., Clausen, B.E., Kaisho, T., Tsujimura, T., Terada, N., Förster, I., and Akira, S. (1999). Enhanced Th1 activity and development of chronic enterocolitis in mice devoid of Stat3 in macrophages and neutrophils. Immunity *10*, 39–49.

Theofilopoulos, A.N., Baccala, R., Beutler, B., and Kono, D.H. (2005). Type I interferons (alpha/beta) in immunity and autoimmunity. Annu. Rev. Immunol. *23*, 307–336.

Tweezer-Zaks, N., Rabinovich, E., Lidar, M., and Livneh, A. (2008). Interferon-alpha as a treatment modality for colchicine-resistant familial Mediterranean fever. J. Rheumatol. *35*, 1362–1365.

Van't Wout, J.W., Van der Meer, J.W., Barza, M., and Dinarello, C.A. (1988). Protection of neutropenic mice from lethal *Candida albicans* infection by recombinant interleukin 1. Eur. J. Immunol. *18*, 1143–1146.

Vonk, A.G., Netea, M.G., van Krieken, J.H., Iwakura, Y., van der Meer, J.W., and Kullberg, B.J. (2006). Endogenous interleukin (IL)-1 alpha and IL-1 beta are crucial for host defense against disseminated candidiasis. J. Infect. Dis. *193*, 1419–1426.

Worthington, M., and Hasenclever, H.F. (1972). Effect of an interferon stimulator, polyinosinic: polycytidylic acid, on experimental fungus infections. Infect. Immun. *5*, 199–202.

Zang, Y.C., Skinner, S.M., Robinson, R.R., Li, S., Rivera, V.M., Hutton, G.J., and Zhang, J.Z. (2004). Regulation of differentiation and functional properties of monocytes and monocyte-derived dendritic cells by interferon beta in multiple sclerosis. Mult. Scler. *10*, 499–506.

Molecular Cell
Article

Linear Ubiquitin Assembly Complex Negatively Regulates RIG-I- and TRIM25-Mediated Type I Interferon Induction

Kyung-Soo Inn,[1,2] Michaela U. Gack,[1,2] Fuminori Tokunaga,[3] Mude Shi,[2] Lai-Yee Wong,[1,2] Kazuhiro Iwai,[3,*] and Jae U. Jung[1,2,*]

[1]Department of Molecular Microbiology and Immunology, University of Southern California, Keck School of Medicine, Los Angeles, CA 90033, USA

[2]Department of Microbiology and Molecular Genetics, New England Primate Research Center, Harvard Medical School, 1 Pine Hill Drive, Southborough, MA 01772-9102, USA

[3]Department of Biophysics and Biochemistry, Graduate School of Medicine and Cell Biology and Metabolism Group, Graduate School of Frontier Biosciences, Osaka University, Suita, Osaka 565-0871, Japan

*Correspondence: kiwai@cellbio.med.osaka-u.ac.jp (K.I.), jaeujung@usc.edu (J.U.J.)

DOI 10.1016/j.molcel.2010.12.029

SUMMARY

Upon detection of viral RNA, retinoic acid-inducible gene I (RIG-I) undergoes TRIM25-mediated K63-linked ubiquitination, leading to type I interferon (IFN) production. In this study, we demonstrate that the linear ubiquitin assembly complex (LUBAC), comprised of two RING-IBR-RING (RBR)-containing E3 ligases, HOIL-1L and HOIP, independently targets TRIM25 and RIG-I to effectively suppress virus-induced IFN production. RBR E3 ligase domains of HOIL-1L and HOIP bind and induce proteasomal degradation of TRIM25, whereas the NZF domain of HOIL-1L competes with TRIM25 for RIG-I binding. Consequently, both actions by the HOIL-1L/HOIP LUBAC potently inhibit RIG-I ubiquitination and antiviral activity, but in a mechanistically separate manner. Conversely, the genetic deletion or depletion of HOIL-1L and HOIP robustly enhances virus-induced type I IFN production. Taken together, the HOIL-1L/HOIP LUBAC specifically suppresses RIG-I ubiquitination and activation by inducing TRIM25 degradation and inhibiting TRIM25 interaction with RIG-I, resulting in the comprehensive suppression of the IFN-mediated antiviral signaling pathway.

INTRODUCTION

The host has evolved at least two classes of pattern recognition receptors (PRRs) that differ fundamentally with respect to their cellular localization to detect viruses: the transmembrane-localized Toll-like receptors (TLRs) and the cytosolic retinoic acid-inducible gene-I (RIG-I) and melanoma differentiation-associated gene 5 (MDA5) receptors (Kawai and Akira, 2008). While TLRs detect incoming virions in the endosomes or phagosomes of specialized immune cells, RIG-I and MDA5 sense actively replicating viruses in the cytoplasm of various cell types (Kato et al., 2006; Yoneyama et al., 2004). RIG-I and MDA5 are members of the DExD/H box RNA helicase family, which serve as the primary intracellular sensors for viral RNA and subsequently initiate signaling cascades leading to type I interferon (IFN) production, thereby establishing an antiviral state (Kato et al., 2006; Nakhaei et al., 2009a; Yoneyama et al., 2004). We have recently demonstrated that tripartite motif protein 25 (TRIM25) interacts with the N-terminal caspase recruitment domains (CARDs) of RIG-I, resulting in the effective delivery of the K63-linked ubiquitin moiety to K_{172} of RIG-I (Gack et al., 2007). This gives rise to an efficient interaction with MAVS/VISA/IPS-1/Cardif, a crucial downstream adaptor protein (Kawai et al., 2005; Meylan et al., 2005; Seth et al., 2005; Xu et al., 2005), leading to the recruitment of signaling molecules such as the TBK1 complex to MAVS. Recruited signaling molecules then activate IRF3 and NF-κB transcription factors to induce IFN production. A recent study also demonstrates that TRIM25 can activate RIG-I in an in vitro reconstituted cell-free system (Zeng et al., 2010).

As seen with TRIM25, the ubiquitination system plays an important role in the regulation of IFN signal transduction (Bhoj and Chen, 2009). In polyubiquitin chains, ubiquitin monomers are usually linked via isopeptide bonds between an internal lysine of one monomer and the C-terminal glycine of the other monomer (Pickart and Fushman, 2004). Recently, a protein complex consisting of two RING finger proteins, HOIL-1L and HOIP, has been shown to exhibit a unique ubiquitin polymerization activity, forming ubiquitin polymers not by lysine linkages, but by linkages between the C and N termini of ubiquitin molecules, to assemble a head-to-tail linear polyubiquitin chain. Thus, this complex is designated as LUBAC (linear ubiquitin assembly complex) (Kirisako et al., 2006). Recent studies have demonstrated that LUBAC activates the canonical NF-κB pathway by binding to NEMO (NF-κ essential modulator, also called IKKγ) to conjugate linear polyubiquitin chains in an Ubc13-independent manner (Rahighi et al., 2009; Tokunaga et al., 2009).

Tight regulation of the immune signaling pathways is essential for a successful immune response against viral infections. Whereas positive regulatory mechanisms lead to the rapid

activation of IFN signaling upon viral infection, negative regulatory mechanisms are required to prevent unwanted or excessive production of IFNs or proinflammatory cytokines. In this report, we unveil the potential feedback inhibitory role of the HOIL-1L/HOIP LUBAC complex through the downregulation of TRIM25 protein level as well as its competition with TRIM25 for RIG-I binding, which ultimately leads to the suppression of the K63-linked ubiquitination and signaling activity of RIG-I.

RESULTS

HOIL-1L/HOIP LUBAC Independently Targets TRIM25 and RIG-I

A yeast two-hybrid screen using a TRIM25 mutant lacking the N-terminal RING domain (TRIM25 ΔRING) as bait revealed that HOIL-1L, a member of the RING-IBR-RING (RBR) E3 ligase family, is a binding partner of TRIM25. Coimmunoprecipitation (coIP) showed that TRIM25 strongly interacts with HOIL-1L (Figure 1A). Due to its significant similarity to HOIL-1L, HOIP also showed a strong interaction with TRIM25 (Figure 1B). To determine whether HOIL-1L and HOIP also interact with RIG-I, HEK293T cells were transfected with a mammalian glutathione S-transferase-RIG-I-2CARD (GST-RIG-I-2CARD) fusion construct together with HOIL-1L and/or HOIP, followed by GST pull-down or coIP assay. This showed that RIG-I efficiently binds to HOIL-1L but not HOIP when they are individually expressed, while coexpression of HOIL-1L and HOIP enables RIG-I to interact with HOIP (Figures 1C and 1D), suggesting that the HOIP and RIG-I-2CARD interaction is mediated by HOIL-1L.

We further examined the interactions between endogenous TRIM25 and RIG-I with HOIL-1L and HOIP in mouse embryonic fibroblast cells (MEFs). Since Sendai virus (SeV) infection readily induces RIG-I-mediated type I IFN signaling, we performed coIP assays with or without SeV infection. RIG-I interactions with HOIL-1L or HOIP were apparent in normal conditions, and these interactions were significantly enhanced by SeV infection (Figure 1E). In contrast, TRIM25 interactions with HOIL-1L or HOIP were detected only after SeV infection (Figure 1E). Confocal microscopy analysis showed that upon viral infection, endogenous HOIL-1L and HOIP have diffuse and punctate patterns in the cytoplasm, where they apparently colocalize with endogenous TRIM25 (Figure 1F). These results collectively show that TRIM25 and RIG-I independently interact with HOIL-1L and HOIP in different manners.

HOIL-1L and HOIP share an Npl4-type zinc finger domain (NZF) and a C-terminal RBR domain, whereas HOIL-1L and HOIP carry the ubiquitin-like (UBL) domain and the ubiquitin-associated (UBA) domain, respectively, which are responsible for their interaction (Kirisako et al., 2006) (Figure S1A). Mutational analysis showed that the C-terminal SPRY domain of TRIM25 is responsible for its interaction with either HOIL-1L or HOIP, whereas the N-terminal two CARDs of RIG-I sufficiently interacted with HOIL-1L (Figures 1G and 1C). To map the regions of HOIL-1L and HOIP responsible for their interactions with TRIM25 and RIG-I, various deletion mutants of HOIL-1L and HOIP were constructed and tested for their ability to bind to TRIM25 and RIG-I. Both HOIL-1L ΔRBR and HOIP ΔRBR, which lack their respective RBR domains, lost their TRIM25 binding abilities (Figure 1H). Interestingly, the HOIP ΔUBA mutant that no longer forms a complex with HOIL-1L was still able to interact with TRIM25 (Figure 1H). Furthermore, not only was TRIM25 and HOIP interaction detected in *HOIL-1L*$^{-/-}$ MEFs (Figure S1B), but a bacterially purified TRIM25 also bound in vitro translated HOIL-1L or HOIP (Figure S1C). These indicate that HOIP interacts with TRIM25 in a HOIL-1L-independent manner.

While the C-terminal RBR domain of HOIL-1L was required for TRIM25 interaction, the central NZF domain of HOIL-1L was necessary for RIG-I interaction (Figure 1H). Consistent with this, HOIL-1L and RIG-I binding was detected in *TRIM25*$^{-/-}$ MEFs, and a yeast two-hybrid screen of HOIL-1L ΔRBR also revealed RIG-I as a binding partner (Figure 1I and data not shown). RIG-I-2CARD readily bound bacterially purified HOIL-1L ΔRBR but showed little or no interaction with HOIP ΔRBR in an in vitro binding assay (Figure 1J). Furthermore, the apparent interaction between HOIL-1L and the RIG-I-2CARD $K_{172}R$ mutant that no longer undergoes K63-linked ubiquitination (Gack et al., 2007) suggests that RIG-I ubiquitination is not required for this interaction (Figure S1D). Finally, unlike TRIM25 binding, for which the first CARD of RIG-I is sufficient (Gack et al., 2008), HOIL-1L binding requires both the first and second CARD of RIG-I (Figure S1E). These results collectively indicate that HOIL-1L and HOIP interact with TRIM25 and RIG-I in distinct manners.

HOIL-1L/HOIP Complex Negatively Regulates RIG-I-Mediated Type I IFN Induction

Either HOIL-1L or HOIP markedly inhibited the IFN-β and NF-κB promoter activity induced by RIG-I-2CARD, a constitutively active form of RIG-I, in a dose-dependent manner (Figures 2A and 2B). Accordingly, HOIL-1L or HOIP expression also suppressed the IFN-β promoter activation induced by a full-length RIG-I upon SeV infection (Figure 2C). To test the effect of HOIL-1L and HOIP on TRIM25-mediated activation of RIG-I, IFN-β, NF-κB, or ISRE, promoter activities were measured from cells transfected with RIG-I, TRIM25, HOIL-1L, and/or HOIP. This showed that HOIL-1L or HOIP effectively nullified the TRIM25 ability to induce RIG-I-mediated IFN-β, NF-κB, or ISRE promoter activation (Figures 2D–2F).

In order to further dissect the role of LUBAC in the negative regulation of the RIG-I signaling, induction of the IFN-β promoter activity was examined in WT, *HOIL-1L*$^{-/-}$, lentiviral shRNA-mediated HOIP knockdown (HOIP KD), and *HOIL-1L*$^{-/-}$-HOIP KD MEFs upon SeV infection (Figure 3A). Upon SeV infection, *HOIL-1L*$^{-/-}$ and *HOIL-1L*$^{-/-}$-HOIP KD MEFs showed markedly increased levels of IFN-β promoter activity compared to WT MEFs. HOIP KD MEFs also showed 2–3 times higher IFN-β promoter activity than WT MEFs (Figure 3B). Consistently, IFN-β production in response to SeV infection was significantly elevated in *HOIL-1L*$^{-/-}$ and *HOIL-1L*$^{-/-}$-HOIP KD MEFs compared to WT MEFs (Figure 3C). In addition, the increased IFN-β response in *HOIL-1L*$^{-/-}$ cells was abrogated by HOIL-1L complementation (Figure 3D). When infected with VSV-eGFP, *HOIL-1L*$^{-/-}$ and *HOIL-1L*$^{-/-}$-HOIP KD MEFs showed substantially fewer VSV-eGFP-positive cells and lower VSV yields (over 10^3- to 10^4-fold) compared with WT MEFs (Figure 3E).

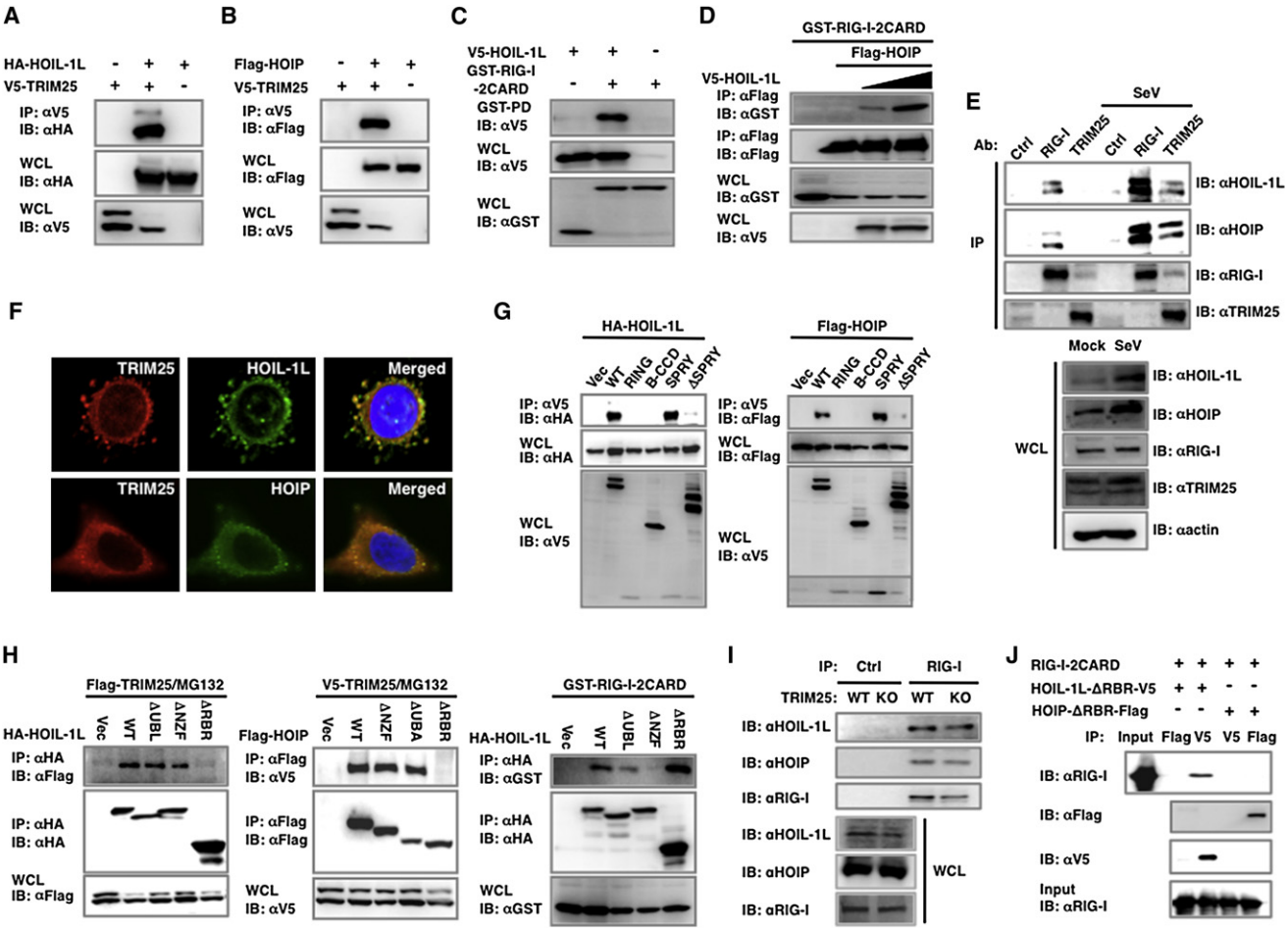

Figure 1. HOIL-1L/HOIP Interacts with TRIM25 and RIG-I

(A and B) Interactions between TRIM25 and HOIL-1L or HOIP. 293T cells were transfected with V5-TRIM25 together with HA-HOIL-1L (A) or Flag-HOIP (B), followed by coIP and IB.

(C) HOIL-1L interacts with RIG-I. 293T cells transfected with GST-RIG-2CARD and V5-HOIL-1L or vector were used for GST pull-down (PD) assay and IB.

(D) HOIP requires HOIL-1L to interact with RIG-I. GST-RIG-2CARD and Flag-HOIP were transfected with increasing amounts of HOIL-1L, followed by IP with anti-Flag.

(E) Endogenous HOIL-1L/HOIP interacts with RIG-I and TRIM25. WT MEFs were mock infected or infected with SeV for 6 hr and treated with MG132 for 4 hr before harvest, followed by IP with control IgG, anti-RIG-I, or anti-TRIM25.

(F) Colocalization of HOIL-1L/HOIP with TRIM25. HeLa cells were mock treated or infected with SeV for 10 hr, followed by fixation and staining with anti-TRIM25, anti-HOIL-1L, or anti-HOIP antibody. Colocalization between TRIM25 and HOIL-1L, Pearson's correlation = 0.871 and Mander's overlap = 0.885; colocalization between TRIM25 and HOIP, Pearson's correlation = 0.702 and Mander's overlap = 0.955.

(G) TRIM25 SPRY domain is responsible for HOIL-1L/HOIP interaction. HA-HOIL-1L or Flag-HOIP was transfected with TRIM25 deletion mutants, followed by coIP.

(H) Binding ability of HOIL-1L or HOIP mutants. Deletion mutants of HOIL-1L or HOIP were transfected with TRIM25 or GST-RIG-I 2CARD as indicated. Cells were treated with MG132 for 6 hr, followed by coIP and IB.

(I) RIG-I interaction with HOIL-1L/HOIP in *TRIM25*$^{-/-}$ MEFs. WT and *TRIM25*$^{-/-}$ MEFs were infected with SeV for 10 hr, followed by coIP using control IgG or anti-RIG-I.

(J) In vitro interaction between RIG-I-2CARD and HOIL-1L. Bacterially purified GST fusion proteins of RIG-I-2CARD, HOIL-1L ΔRBR-V5, and HOIP ΔRBR-Flag were used for in vitro binding, followed by coIP and IB as indicated. See also Figure S1.

Accordingly, the HOIL-1L complementation of *HOIL-1L*$^{-/-}$ MEFs led to the robust recovery of VSV-eGFP replication. Moreover, HOIL-1L overexpression also led to the drastic increase of VSV-eGFP replication (Figures 3F and 3G). Collectively, these results indicate that LUBAC serves as a critical negative regulator of the RIG-I-mediated antiviral IFN response.

HOIL-1L/HOIP LUBAC Reduces the TRIM25-Induced K63-Linked Ubiquitination of RIG-I

Next, we tested whether HOIL-1L/HOIP LUBAC affects the TRIM25-mediated RIG-I ubiquitination and thereby suppresses its downstream signaling activity. GST-RIG-I-2CARD and TRIM25 were coexpressed together with increasing amounts

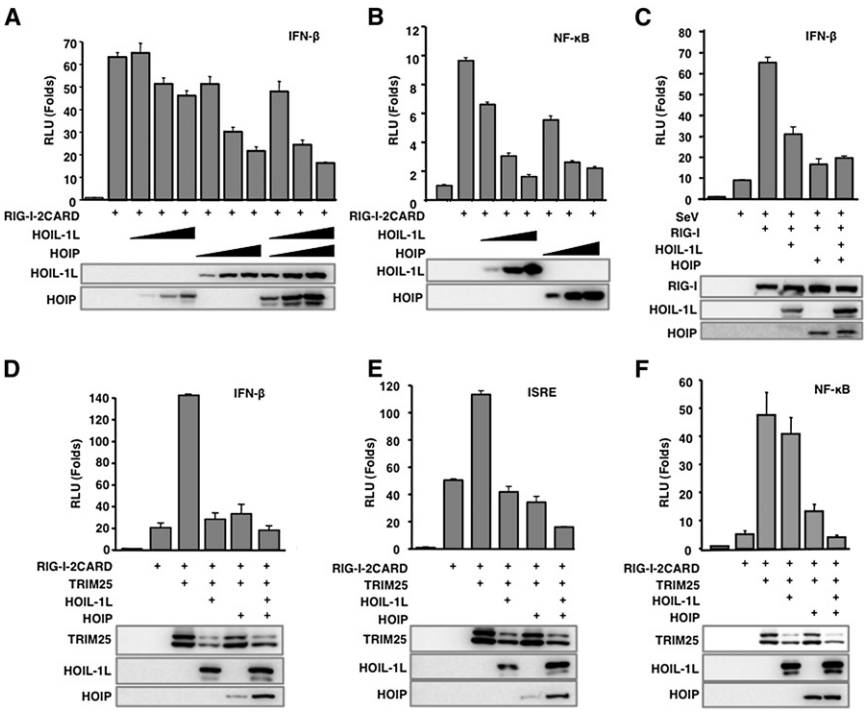

Figure 2. HOIL-1L/HOIP Complex Negatively Regulates RIG-I-Mediated IFN-β Signaling

(A and B) Inhibition of RIG-I-2CARD induced IFN-β and NF-κB promoter activities by HOIL-1L/HOIP. 293T cells were transfected with RIG-I-2CARD with increasing amounts of HOIL-1L, HOIP, or both together with IFN-β (A) or NF-κB promoter (B).

(C) Inhibition of SeV induced IFN-β promoter activity by HOIL-1L/HOIP. IFN-β promoter activities were measured from 293T cells transfected with full-length RIG-I and HOIL-1L and/or HOIP. At 24 hr after transfection, cells were mock infected or infected with SeV (40 HAU/ml) for 10 hr before luciferase assay.

(D–F) RIG-I-2CARD, TRIM25, HOIL-1L, and HOIP plasmids were transfected together with IFN-β (D), ISRE (E), or NF-κB (F) reporter plasmids into 293T. All luciferase assays were performed at least three times and graphs show the mean ± SD. Values are normalized by pRL-TK Renilla.

of HOIL-1L and/or HOIP. While GST-RIG-I-2CARD underwent robust ubiquitination in the presence of TRIM25 (Gack et al., 2007), its ubiquitination levels were detectably decreased by either the individual expression of HOIL-1L or HOIP or further reduced by HOIL-1L and HOIP coexpression (Figures 4A and S2). In line with this, the ubiquitination of endogenous RIG-I was readily detected upon SeV infection, and this ubiquitination was profoundly reduced by HOIL-1L and HOIP overexpression (Figure 4B). Conversely, eliminating the HOIL-1L gene and/or silencing the HOIP gene enhanced the ubiquitination levels of endogenous RIG-I upon viral infection (Figure 4C). Furthermore, immunoblotting with a K63-linked polyubiquitin-specific antibody (Wang et al., 2008) confirmed the increase of K63-linked polyubiquitinated RIG-I in HOIL-1L- or HOIP-depleted cells (Figure 4C). Consistent with the notion that K63-linked RIG-I ubiquitination plays a crucial role for its interaction with MAVS (Gack et al., 2007), HOIL-1L and HOIP expression efficiently inhibited the RIG-I-2CARD and MAVS-CARD interaction (Figure 4D). This indicates that LUBAC suppresses RIG-I ubiquitination, thereby blocking its interaction with MAVS.

HOIL-1L/HOIP LUBAC Induces the Ubiquitination and Degradation of TRIM25

To elaborate the effect of HOIL-1L/HOIP LUBAC on RIG-I and TRIM25 function, we tested whether HOIL-1L and HOIP inhibited RIG-I ubiquitination by lowering the TRIM25 level. We found that SeV-infected HOIP KD MEFs had a greater amount of endogenous TRIM25 compared to WT MEFs, with the highest levels found in *HOIL-1L*$^{-/-}$-HOIP KD MEFs (Figure 5A). Conversely, HOIL-1L and/or HOIP expression led to a measurable reduction of endogenous TRIM25 (Figure 5B). Transient expression assay also showed that HOIL-1L and HOIP coexpression induced a detectable reduction of TRIM25 in a synergistic manner, but this reduction was efficiently reversed by MG132 proteasome inhibitor treatment (Figure 5C). In addition, HOIL-1L and HOIP expression increased the level of TRIM25 ubiquitination, which was more pronounced upon MG132 treatment (Figure 5D). While TRIM25 ubiquitination was potently induced in WT MEFs upon SeV infection, it was markedly reduced in HOIL-1L-depleted and/or HOIP-depleted MEFs (Figures 5E and 5F). Furthermore, TRIM25 ubiquitination was dependent on the HOIL-1L and HOIP E3 ligase activities, as mutating the conserved cysteines in the RING domains of HOIL-1L and HOIP into serine (RING^{CS}) rendered them unable to ubiquitinate TRIM25 (Figure 5G). Finally, the LUBAC-mediated degradation of TRIM25 was specific, since LUBAC showed little or no effect on ectopically expressed RIG-I levels (Figure S3A). It should be noted that due to its negative role in IFN signal transduction, HOIL-1L/HOIP LUBAC expression affects the RIG-I mRNA and protein levels induced by SeV infection, as seen with IFN-β (Figures 4B, 4C, and S3B).

An in vitro ubiquitination assay showed that the HOIL-1L/HOIP LUBAC purified from a baculovirus expression system specifically ubiquitinated bacterially purified GST-TRIM25 RING^{CS}, but not GST-RIG-2CARD (Figures 5H and S3C). The TRIM25 ΔSPRY mutant, lacking the C-terminal SPRY domain and thereby no longer interacting with HOIL-1L and HOIP, did not undergo ubiquitination upon viral infection (Figure S3D). Conversely, the TRIM25 SPRY domain alone, which is sufficient to interact with HOIL-1L and HOIP, underwent robust ubiquitination that was decreased upon shRNA-mediated knockdown of HOIL-1L or HOIP gene expression (Figures S3E–S3H). The Lys48 (K48)-linked ubiquitin chain was the original type identified; however, more recent works have uncovered a wide variety of linkages, including K63-linked and linear ubiquitin chains

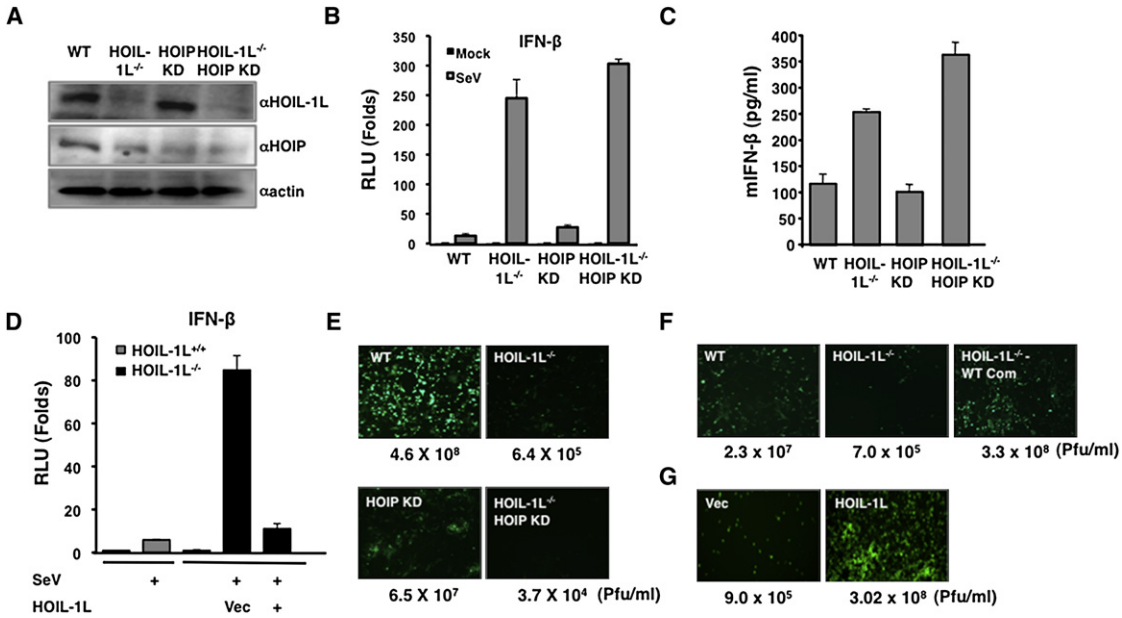

Figure 3. HOIL-1L/HOIP Depletion Increases IFN-β Production and Antiviral Response

(A) WT, *HOIL-1L*$^{-/-}$, HOIP knockdown MEF (HOIP KD), and *HOIL-1L*$^{-/-}$-HOIP KD MEFs were established as described in the Experimental Procedures. Depletion and reduction of HOIL-1L and HOIP, respectively, were confirmed by IB.

(B) Enhanced IFN-β promoter activity in HOIL-1L/HOIP-depleted MEFs. MEFs were infected with SeV (50 HAU/ml) for 10 hr and then subjected to dual luciferase assay. Experiments were performed in triplicate, and graph shows the mean ± SD.

(C) Increased IFN-β production in HOIL-1L/HOIP-depleted MEFs. MEFs were infected with SeV (50 HAU/ml) for 12 hr and supernatants were subjected to mouse IFN-β ELISA. Experiments were performed in triplicate, and graph shows the mean ± SD.

(D) Suppression of IFN-β promoter activity in *HOIL-1L*$^{-/-}$ MEFs by complementation of HOIL-1L. HOIL-1L was cotransfected with reporter plasmid as indicated. Virus infection and luciferase assay were performed similarly to (A). Experiments were performed in triplicate, and graph shows the mean ± SD.

(E and F) Viral replication in HOIL-1L/HOIP-depleted MEFs. MEFs were infected with VSV-eGFP (moi = 0.02). Supernatants were taken at 48 hr p.i. and subjected to plaque assay.

(G) VSV-eGFP replication in 293T expressing vector alone or HOIL-1L.

(Ikeda and Dikic, 2008). Since LUBAC is known to generate linear ubiquitination, we tested whether LUBAC can conjugate a linear ubiquitin chain onto TRIM25. An in vitro assay with a ubiquitin KO mutant containing no lysine residues showed that HOIL-1L/HOIP LUBAC was able to efficiently incorporate linear ubiquitin chains onto TRIM25 (Figure S3I). In addition, the linear ubiquitination of TRIM25 was detectably increased upon SeV infection or ectopic expression of HOIL-1L/HOIP LUBAC (Figure S3J). Furthermore, TRIM25 also underwent K48-linked ubiquitination upon SeV infection, which was significantly attenuated by shRNA-mediated knockdown of HOIP expression (Figure S3K). Conversely, HOIL-1L/HOIP LUBAC expression induced the K48-linked ubiquitination of TRIM25, which was further augmented by treatment with MG132 (Figure S3L). In contrast, K63-linked ubiquitination of TRIM25 was not detected in vivo (Figure S3K and data not shown).

TRIM25 Undergoes Self-Monoubiquitination

It was noted that TRIM25 WT, but not the TRIM25^{CS} E3 ligase dead mutant, was present as a doublet (70 and 78 kDa) and that the upper band of TRIM25 often disappeared upon HOIL-1L and HOIP expression (Figures 1A, 1B, and S3M), suggesting that TRIM25 undergoes automonoubiquitination and that the monoubiquitinated form of TRIM25 may be highly susceptible to HOIL-1L and HOIP. Mass spectrometry showed that the upper band of TRIM25 is monoubiquitinated at the K_{117}, K_{264}, K_{320}, and K_{416} residues. To corroborate the monoubiquitination of TRIM25, we individually replaced these four lysine residues with arginine (K → R) and then tested these mutants for their ubiquitination levels. The K_{117}R mutation of TRIM25 caused the near-complete loss of monoubiquitination, whereas the K_{264}R, K_{320}R, and K_{416}R mutations led to little or no reduction of monoubiquitination (Figures S3N). Intriguingly, the TRIM25 K_{117}R mutant was functionally similar to WT TRIM25 with respect to its ability to ubiquitinate RIG-I-2CARD and induce RIG-I-mediated IFN-β promoter activation (Figures S3O and S3P). Furthermore, the TRIM25 K_{117}R mutant was still sensitive to the ubiquitination and signaling inhibition induced by the HOIL-1L/HOIP LUBAC (Figures S3Q and S3R). These data indicate that the monoubiquitination of TRIM25 is not essential for its RIG-I activation function and that LUBAC targets both non- and monoubiquitinated forms of TRIM25.

HOIL-1L/HOIP LUBAC Complex Interrupts the Interaction between TRIM25 and RIG-I

To determine whether the E3 ligase activities of HOIL-1L and HOIP are sufficient to negatively regulate RIG-I-mediated IFN-β signaling, the HOIL-1L and HOIP RING^{CS} E3-ligase defective

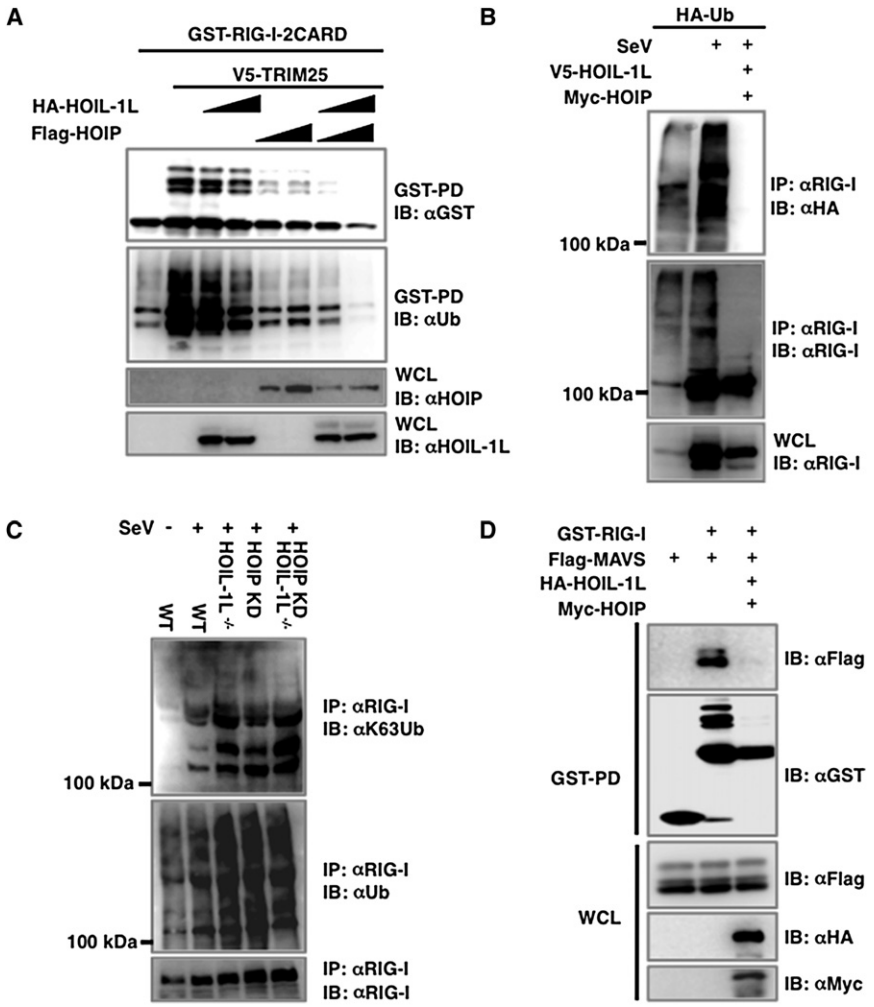

Figure 4. HOIL-1L/HOIP LUBAC Inhibits TRIM25-Mediated RIG-I Ubiquitination

(A) Inhibition of RIG-I ubiquitination by HOIL-1L/HOIP. 293T cells transfected with GST-RIG-I-2CARD and TRIM25 together with HOIL-1L or HOIP were subjected to GST-PD and IB.

(B) Inhibition of endogenous RIG-I ubiquitination by HOIL-1L/HOIP. 293T cells transfected with HA-ubiquitin with or without HOIL-1L/HOIP were mock infected or infected with SeV for 10 hr, followed by IP with anti-RIG-I.

(C) RIG-I ubiquitination in HOIL-1L/HOIP-depleted MEFs. WT, *HOIL-1L*$^{-/-}$, HOIP-KD, and *HOIL-1L*$^{-/-}$-HOIP-KD MEFs infected with SeV were used for IP and IB. Anti-ubiquitin (αUb) antibody and anti-K63-ubiquitin chain-specific antibody (αK63) were used to detect RIG-I ubiquitination.

(D) Decreased interaction between RIG-I and MAVS by HOIL-1L/HOIP expression. 293T cells transfected with Flag-RIG-I-2CARD, GST-MAVS-CARD-proline-rich domain (PRD), V5-HOIL-1L, and/or Myc-HOIP were used for coIP and IB. See also Figure S2.

mutants were tested for their abilities to downregulate RIG-I ubiquitination and IFN-β signaling. Surprisingly, the RING^{CS} mutants of both HOIL-1L and HOIP still suppressed SeV- or RIG-I-induced IFN-β promoter activation and TRIM25-mediated RIG-I ubiquitination (Figures S4A, S4B, and 6A), suggesting that HOIP/HOIL-1L LUBAC might have additional mechanisms to downregulate RIG-I ubiquitination and signaling activity other than TRIM25 degradation. We hypothesized that the diverse interacting activities of HOIL-1L and HOIP could ultimately influence the interaction between TRIM25 and RIG-I. Indeed, the interaction between RIG-I-2CARD and TRIM25 was noticeably reduced by HOIL-1L or HOIP expression where the reduction was further decreased by HOIL-1L and HOIP coexpression (Figure 6B, left). Moreover, increasing levels of HOIL-1L and HOIP coexpression inhibited the interaction between RIG-I-2CARD and TRIM25 in a dose-dependent manner (Figure 6B, right). Conversely, the interaction between endogenous RIG-I and TRIM25 was elevated in *HOIL-1L*$^{-/-}$ MEFs and *HOIL-1L*$^{-/-}$-HOIP KD MEFs (Figure 6C). The interaction between endogenous RIG-I and TRIM25 reached a peak at 8 hr after SeV infection and declined afterward, coinciding with the significant increase in HOIL-1L and HOIP protein levels after 12 hr of SeV infection (Figure 6D). These results were further confirmed in in vitro binding assays using bacterially purified GST fusions of RIG-2CARD, TRIM25, HOIL-1L ΔRBR, and HOIP ΔRBR. Increasing amounts of LUBAC ΔRBR (HOIL-1L ΔRBR/HOIP ΔRBR) proteins led to the decreased interaction between RIG-I-2CARD and TRIM25 in a dose-dependent manner, while the interaction between RIG-I and LUBAC ΔRBR increased under the same conditions (Figure 6E).

To further analyze this binding competition, biotin-labeled GST-TRIM25 was added to immobilized GST-RIG-I-2CARD, followed by the addition of increasing amounts of unlabeled TRIM25 or LUBAC ΔRBR (HOIL-1L ΔRBR/HOIP ΔRBR) as binding competitors. Biotin-labeled TRIM25 interaction with RIG-I-2CARD was inhibited by unlabeled TRIM25 or LUBAC ΔRBR to similar extent, suggesting that TRIM25 and LUBAC may have similar binding affinities to RIG-I (Figure 6F). On the other hand, the HOIL-1L ΔNZF mutant, which does not interact with RIG-I, failed to compete with TRIM25 for RIG-I-2CARD binding (Figure S5A). Consequently, the HOIL-1L ΔNZF mutant downregulated RIG-I ubiquitination and IFN-β promoter activation to a much lesser extent than HOIL-1L WT (Figures S5B and S5C). Interestingly, the HOIL-1L ΔUBL mutant that lost the LUBAC formation with HOIP only weakly inhibited RIG-I ubiquitination and signaling activity compared to its wild-type, suggesting that the LUBAC formation between HOIL-1L and HOIP is important for its suppressive activity (Figures S5B and S5C).

To further corroborate the importance of HOIL-1L NZF domain for RIG-I inhibition, we generated the NZF^{CS} mutant that lost its zinc finger structure due to the mutations of the conserved

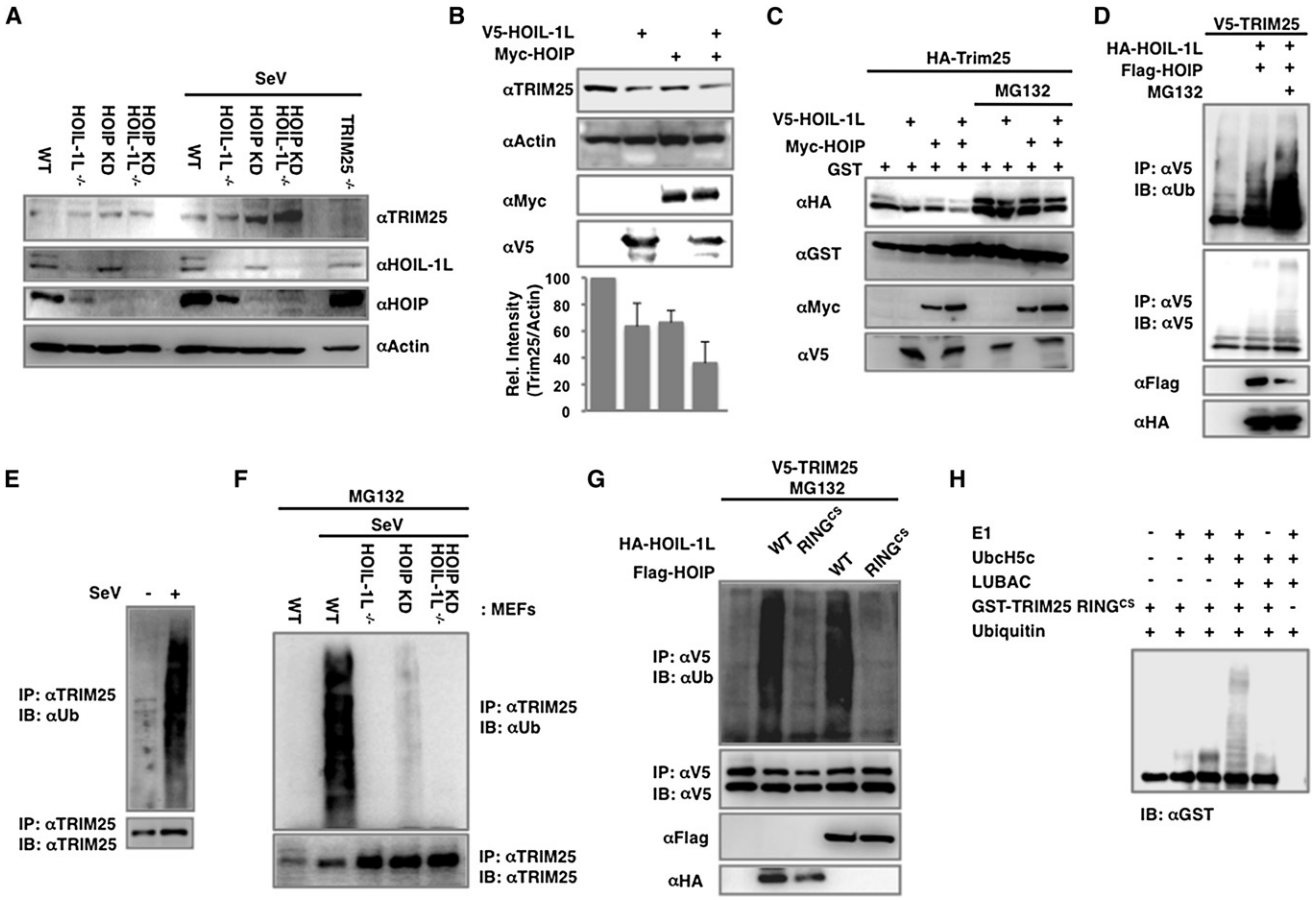

Figure 5. HOIL-1L/HOIP LUBAC Induces TRIM25 Ubiquitination and Degradation

(A) Increment of TRIM25 levels in HOIL-1L/HOIP-depleted MEFs. WT, *HOIL-1L*$^{-/-}$, HOIP KD, and *HOIL-1L*$^{-/-}$-HOIP KD MEFs were mock infected or infected with SeV for 12 hr. Cell lysates were subjected to IB.

(B) Decreased endogenous TRIM25 levels upon HOIL-1L/HOIP overexpression. Endogenous TRIM25 levels were analyzed by IB and densitometry. IBs show representative data, and graph shows the averages of triplicate.

(C) Reduction of TRIM25 by HOIL-1L/HOIP expression. At 36 hr after the transfection with V5-TRIM25 and GST together with HOIL-1L and HOIP as indicated, 293T cells were mock treated or treated with MG132 for 6 hr and subjected to IB.

(D) TRIM25 ubiquitination induced by HOIL-1L/HOIP. 293T cells were transfected with V5-TRIM25, HOIL-1L, and HOIP and MG132 treatment for IP.

(E) Endogenous TRIM25 ubiquitination upon SeV infection. MEFs were mock infected or infected with SeV for 10 hr, and cell lysates were subjected to IP using anti-TRIM25 antibody.

(F) TRIM25 ubiquitination levels in HOIL-1L/HOIP-depleted MEFs. MEFs were infected with SeV and treated with MG132, followed by IP with anti-TRIM25 and IB with anti-Ub or anti-TRIM25.

(G) TRIM25 ubiquitination by HOIL-1L/HOIP RING^{CS} mutants. 293T cells were transfected with V5-TRIM25 and WT or RING^{CS} mutants of HOIL-1L or HOIP, followed by IP with anti-V5 and IB with anti-Ub or anti-V5.

(H) In vitro ubiquitination of TRIM25 by LUBAC. Purified GST-TRIM25 RING^{CS} was subjected to an in vitro ubiquitination with baculovirus-purified HOIL-1L/HOIP LUBAC, followed by IB with anti-GST antibody. See also Figure S3.

cysteines to serines. As seen with its ΔNZF mutant, HOIL-1L NZF^{CS} mutant did not bind to RIG-I-2CARD (Figure 7A). Consequently, HOIL-1L NZF^{CS} mutant was incapable of suppressing the interaction between RIG-I and TRIM25 (Figure 7B) and thus showed reduced ability to downregulate RIG-I ubiquitination and IFN-β promoter activation (Figures 7C and 7D). These results suggest that HOIL-1L suppresses the RIG-I-TRIM25 interaction by binding RIG-I in a competitive fashion, resulting in an inhibitory effect on RIG-I signaling activity.

Finally, *HOIL-1L*$^{-/-}$ MEFs were complemented with wild-type HOIL-1L or its mutants (NZF^{CS} or RING^{CS}) and subsequently infected with SeV to measure IFN-β promoter activity and production. A high basal level of SeV infection-induced IFN-β production of *HOIL-1L*$^{-/-}$ MEFs was robustly dampened by complementation with the HOIL-1L WT (Figure 7E). In contrast, the complementation with either the HOIL-1L NZF^{CS} or the HOIL-1L RING^{CS} mutant resulted in significantly weaker suppression of antiviral response than that with the HOIL-1L WT as assayed by IFN-β promoter activity and IFN-β production (Figures 7E and 7F). These data collectively demonstrate that LUBAC comprehensively suppresses RIG-I antiviral activity by inducing the C-terminal RBR-E3 ligase-mediated degradation of TRIM25

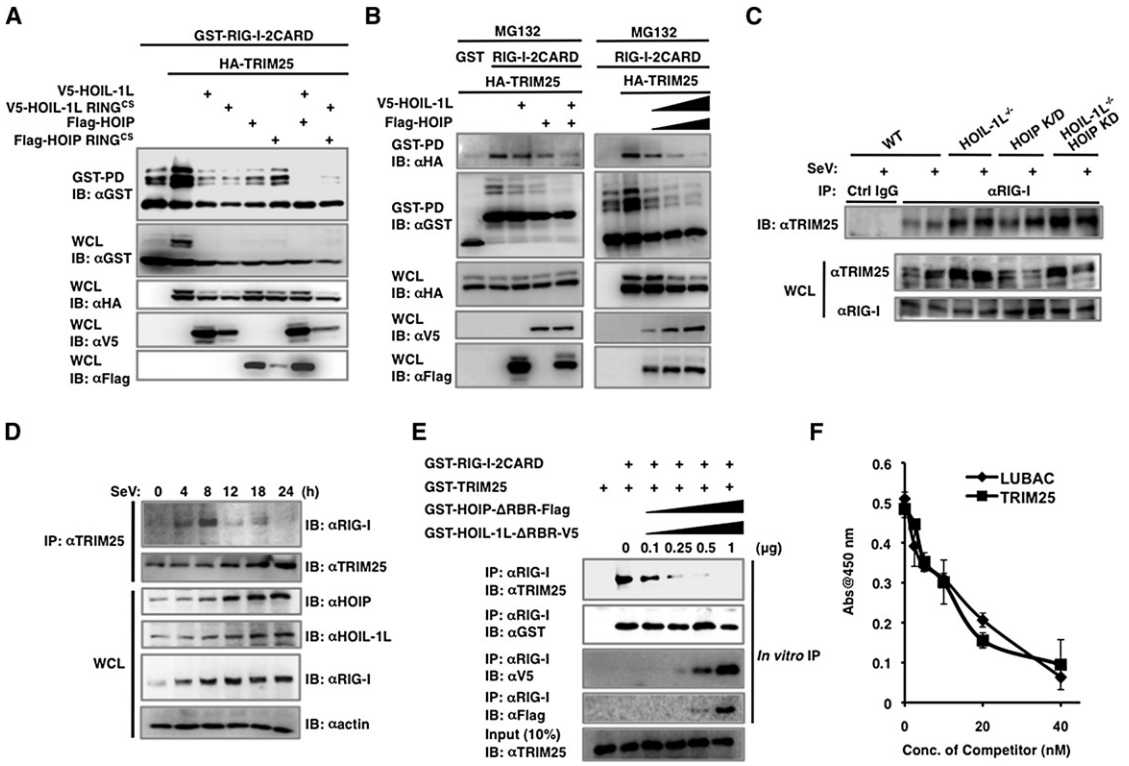

Figure 6. HOIL-1L/HOIP LUBAC Inhibits the Interaction between RIG-I and TRIM25

(A) Inhibition of RIG-I ubiquitination by HOIL-1L/HOIP RING^{CS} mutants. 293T cells were transfected with GST-RIG-I-2CARD and TRIM25 together with HOIL-1L, HOIP, or RING^{CS} mutants and treated with MG132, followed by GST-PD.

(B) Inhibition of RIG-I-2CARD and TRIM25 interaction by HOIL-1L/HOIP. 293T cells were transfected with GST-RIG-I-2CARD and TRIM25 together with HOIL-1L and/or HOIP as indicated, followed by GST-PD.

(C) Increased interaction between RIG-I and TRIM25 in HOIL-1L/HOIP-depleted MEFs. MEFs were mock infected or infected with SeV (50 HAU/ml) for 12 hr and subjected to coIP using control IgG or anti-RIG-I.

(D) Time course analysis of endogenous RIG-I and TRIM25 interaction. At different time points after SeV infection, the same amounts of proteins from WT MEFs were subjected to coIP using anti-TRIM25.

(E) In vitro competition assay. Bacterially purified GST-RIG-I-2CARD and GST-TRIM25 were incubated with increasing amounts of GST-HOIL-1L ΔRBR-V5 or GST-HOIP ΔRBR-Flag, followed by IP with anti-RIG-I.

(F) Inhibition of RIG-I and TRIM25 interaction by LUBAC. Biotin-labeled GST-TRIM25 were added to GST-RIG-I-coated wells with increasing amounts of GST-HOIL-1L ΔRBR-V5/GST-HOIP ΔRBR-Flag (LUBAC) or unlabeled GST-TRIM25. Bound, biotin-labeled GST-TRIM25 was detected using streptavidin-HRP. Experiments were performed in triplicate, and graph shows the mean ± SD. See also Figure S4.

and the central NZF-mediated inhibition of TRIM25-RIG-I interaction (Figure 7G).

DISCUSSION

Tight regulation of immune signaling pathways is essential for a successful immune response against viral infections; otherwise, excessive production of IFNs or proinflammatory cytokines would be destructive rather than protective. In this report, we unveil the potential feedback inhibitory role of the HOIL-1L/HOIP LUBAC, which specifically suppresses RIG-I ubiquitination and activation by inducing TRIM25 degradation and inhibiting TRIM25 and RIG-I interaction.

Similar to the HOIL-1L/HOIP LUBAC, numerous intracellular proteins have been demonstrated to contribute to the negative regulation or feedback inhibition of RIG-I signal transduction. First, the RIG-I-like RNA helicase, Lgp2, which lacks the CARD domains, inhibits virus-induced RIG-I downstream signaling (Komuro and Horvath, 2006; Rothenfusser et al., 2005), and RNF125 E3 ligase catalyzes RIG-I proteasomal degradation (Arimoto et al., 2007), whereas CYLD deubiquitinase eliminates the K63-linked polyubiquitin chain from RIG-I to downregulate its signaling activity (Friedman et al., 2008). In addition, A20, NLRX1, PIN1, DUBA, and Triad3A deregulate RIG-I-mediated signaling by inhibiting MAVS, IRF3, and TRAF3 (Kayagaki et al., 2007; Lin et al., 2006; Moore et al., 2008; Nakhaei et al., 2009b; Saitoh et al., 2006). Furthermore, the alternative splicing or ISGylation of RIG-I also negatively regulates its function on virus-triggered IFN production (Gack et al., 2008; Kim et al., 2008). Finally, the influenza A virus nonstructural protein 1 (NS1) specifically inhibits TRIM25-mediated RIG-I ubiquitination, thereby suppressing RIG-I signal transduction (Gack et al., 2009). This indicates that the host dedicates a number of its intracellular components to tightly

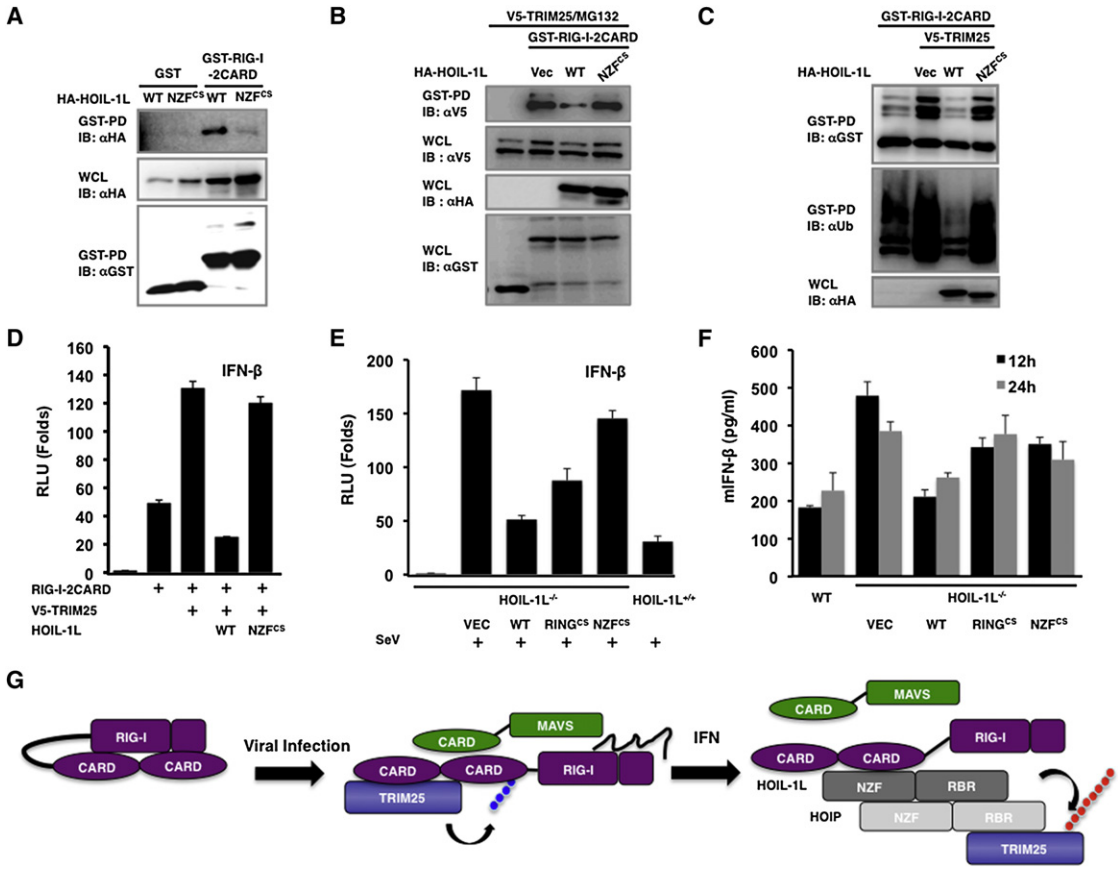

Figure 7. Roles of the NZF and RBR Domains of HOIL-1L in RIG-I-Mediated IFN-β Signaling

(A) Inability of HOIL-1L NZF^{CS} mutant to bind RIG-I. 293T cells were transfected with GST-RIG-I-2CARD together with HA-HOIL-1L WT or NZF^{CS} mutant, followed by GST-PD and IB with indicated antibodies.

(B) Inability of HOIL-1L NZF^{CS} mutant to interfere the RIG-I-TRIM25 interaction. 293T cells were transfected with GST-RIG-I-2CARD and TRIM25 together with HA-HOIL-1L WT or NZF^{CS} mutants and treated with MG132, followed by GST-PD and IB.

(C) Inability of HOIL-1L NZF^{CS} mutant to inhibit RIG-I ubiquitination. 293T cells were transfected with GST-RIG-I-2CARD and TRIM25 together with HOIL-1L WT or NZF^{CS} mutant as indicated, followed by GST-PD and IB.

(D) Effect of HOIL-1L WT or NZF^{CS} mutant on RIG-I-mediated IFN-β promoter activity. IFN-β promoter activities were determined from 293T cells transfected with RIG-I-2CARD and TRIM25 together with HOIL-1L WT or NZF^{CS} mutant. Experiments were performed in triplicate, and graph shows the mean ± SD.

(E and F) Complementation of *HOIL-1L*$^{-/-}$ MEFs. *HOIL-1L*$^{-/-}$ MEFs were infected with recombinant retrovirus containing HOIL-1L WT, RING^{CS}, or NZF^{CS} mutant, followed by the puromycin antibiotic selection. Complemented MEFs were transfected with IFN-β reporter, followed by mock infection or SeV infection and luciferase assay (E). Experiments in (E) were performed in triplicate, and graph shows the mean ± SD. Complemented MEFs were mock infected or infected with SeV (50 HAU/ml), and supernatants were subjected to IFN-β ELISA (F). Experiments in (F) were performed in triplicate, and graph shows the mean ± SD.

(G) Hypothetical model for LUBAC-mediated inhibition of RIG-I and TRIM25 pathway. See also Figure S5.

control RIG-I signaling for the successful elimination of viral infections.

Mutational analysis showed that the C-terminal RBR domains of HOIL-1L and HOIP are essential for TRIM25 binding, whereas the central NZF domain of HOIL-1L is necessary for RIG-I binding, indicating that HOIL-1L and HOIP interact with TRIM25 and RIG-I in different manners. While the detailed resolution of the HOIL-1L/HOIP LUBAC interactions with TRIM25 or RIG-I need to be further characterized, these differential interactions of HOIL-1L and HOIP with TRIM25 and RIG-I eventually lead to the competition between the LUBAC and TRIM25 for RIG-I binding, resulting in the reduction of the K63 ubiquitination of RIG-I. Furthermore, LUBAC expression induces TRIM25 ubiquitination and proteasomal degradation, thereby suppressing RIG-I-mediated IFN signaling. Conversely, HOIL-1L knockout and HOIP KD cells showed markedly higher IFN production than WT cells, suggesting that LUBAC serves as an important negative factor to tightly control RIG-I signaling activity.

The HOIL-1L/HOIP LUBAC has been shown to negatively regulate various signaling pathways by degrading its interacting partners, such as IRP2, TAB1/2, and Bach1, through ubiquitin-dependent proteasomal pathway (Ishikawa et al., 2005; Tian et al., 2007; Zenke-Kawasaki et al., 2007). In addition, a recent study showed that linear ubiquitination of a protein can lead to its proteasomal degradation (Zhao and Ulrich, 2010). Our study has added TRIM25 into the increasing substrate list of HOIL-1L and HOIP LUBAC. However, both the RING^{CS} and ΔRBR mutants of HOIL-1L and HOIP that lose ubiquitin-incorporating activity were still

capable of downregulating RIG-I signaling, suggesting that LUBAC might have additional mechanism(s) to suppress RIG-I ubiquitination and signaling activity. Indeed, we found that the interaction between HOIL-1L and RIG-I competitively suppresses the interaction between TRIM25 and RIG-I. Particularly, this action is dependent on the central NZF domain of HOIL-1L: the HOIL-1L ΔNZF or NZF^{CS} mutant, which lost RIG-I binding ability, was incapable of suppressing the interaction between RIG-I and TRIM25 and thus showed the reduced activity to downregulate the RIG-I ubiquitination and IFN-β promoter activation. The NZF domain is frequently found in proteins involved in ubiquitin-dependent pathways, such as TAB2, TAB3 (Kanayama et al., 2004), Npl4 (Meyer et al., 2002), and yeast Vps36 (Alam et al., 2004). The ubiquitin-binding NZF domain is comprised of a highly conserved TF/Φ motif, where Φ represents a hydrophobic residue and ten amino acid residues are inserted between the Thr-Phe (TF) sequence and Φ (Alam et al., 2004). Certain NZF domains can discriminate against different types of ubiquitin chains, as exemplified by the NZF domain of TAB2, which displays a high affinity for the K63-linked ubiquitin moiety (Kanayama et al., 2004). It is particularly intriguing that since free, unanchored, K63-linked ubiquitin chain is able to activate RIG-I signaling (Zeng et al., 2010), the NZF domain may potentially function as a K63-linked, ubiquitin chain-anchoring motif for RIG-I signaling. However, while the central NZF domain of HOIL-1L plays an important role in RIG-I CARD binding, this binding is not dependent on the K63-linked ubiquitination of RIG-I CARD. Further structural studies are necessary to delineate the interaction between the N-terminal RIG-I CARD and the central HOIL-1L NZF domain.

During our research, it has been reported that RBCK1, an alternative name of HOIL-1L, downregulates RIG-I signaling through IRF3 degradation in transient overexpression conditions (Zhang et al., 2008). However, we were unable to observe the detectable reduction of endogenous IRF3 levels upon HOIL-1L and/or HOIP transient expression (data not shown) or in *HOIL-1L*$^{-/-}$ MEFs, HOIP KD MEFs, or *HOIL-1L*$^{-/-}$-HOIP KD MEFs (data not shown), suggesting that IRF3 may not be a direct substrate for HOIL-1L/HOIP LUBAC. In summary, our data collectively demonstrate that HOIL-1L/HOIP LUBAC comprehensively suppresses RIG-I antiviral activity by inducing the C-terminal RBR E3 ligase-mediated degradation of TRIM25 and/or the central NZF-mediated inhibition of TRIM25 and RIG-I interaction (Figure 7G). Thus, the HOIL-1L/HOIP complex represents a negative regulator of RIG-I- and TRIM25-mediated innate immunity that may serve to prevent an excessive and prolonged IFN production.

EXPERIMENTAL PROCEDURES

Plasmids

GST-RIG-2CARD, GST-RIG-I 1st CARD, GST-RIG-I 2nd CARD, pBOS-Flag-RIG-I, MAVS-CARD-PRD, pIRES-V5-TRIM25, and its deletion mutants were previously described (Gack et al., 2007). HOIL-1L-His6-HA wild-type, Flag-, Myc-HOIP wild-type, their deletion mutants, and their $RING^{CS}$ and NZF^{CS} mutants were described previously (Kirisako et al., 2006). pBabe-HOIL-1L and mutants for complementation assay were obtained by standard PCR and cloning method.

Antibodies and Other Reagents

Mouse monoclonal antibody 2E2 against HOIL-1L (Kirisako et al., 2006) and anti-linear ubiquitin antibody (Tokunaga et al., 2009) were described previously. Antibodies against TRIM25 (BD Biosciences), RIG-I (mouse monoclonal, Alexis; rabbit, IBL), HOIP (goat, IMGENEX; rabbit, Abcam), MAVS (Cell Signaling), ubiquitin (Santa Cruz, P4D1), K63 polyubiquitin chain (HWA4C4, Biomol), K48 polyubiquitin chain (Apu2, Millipore) and actin (Abcam) were purchased from the indicated manufacturer. VSV-eGFP was described previously (Gack et al., 2007).

Yeast Two-Hybrid Screen

A human B lymphocyte cDNA library was screened using TRIM25 ΔRING as bait. Matchmaker yeast two-hybrid system was obtained from Clontech.

Cell Lines

HOIL-1L$^{-/-}$ MEF cell line was described previously (Tokunaga et al., 2009). HOIP-KD and *HOIL-1L*$^{-/-}$-HOIP KD MEFs were established by stable knockdown of HOIP using shRNA (Open Biosystems; TRCN0000037277; CAGAGAA ACAACGCCAAGATACTCGAGTATCTTGGCGTTGTTTCTCTG). Cells transduced with lentivirus were selected with puromycin (2 μg/ml) 2 days after infection. Control cell lines were generated using scrambled control shRNA vector. HOIL-1L stable-expressing HEK293T cell line was generated by transfecting pcDNA3-HOIL-1L, followed by selection with G418 (400 μg/ml). For the complementation, *HOIL-1L*$^{-/-}$ MEFs were infected with pBabe-HOIL-1L WT or mutant retrovirus, followed by 4 day selection with puromycin.

IFN-β Production and Virus Replication Assay

Cell culture supernatants were collected from cells infected with SeV as indicated in the figure legends and subjected to IFN-β ELISA (PBL Biomedical Laboratories). To assay the viral replication, culture supernatants were collected from VSV-eGFP-infected cells, and viral titer was determined in Vero cells by standard plaque assay.

Reporter Assays

All reporter assays were performed using Dual-Luciferase Assay kit (Promega). Cells were transfected with the indicated reporters together with pRL-TK reporter. Twenty-four hours after transfection, cells were treated as indicated in the figure legends.

Immunoprecipitation and Immunoblot Analysis

For coIPs, cells were lysed with NP40 lysis buffer (25 mM Tris [pH 7.5], 150 mM NaCl, 1 mM EDTA, 0.6% Nonidet P-40). After clarification and preclearing, protein amounts were determined using BCA assay. Cell extracts were incubated for 12–16 hr with the indicated antibodies, followed by further incubation with protein A/G bead for 2–4 hr. The immune complexes were washed with lysis buffer with various concentrations of NaCl and subjected to western blot analysis. For endogenous coIP, antibodies were conjugated to resin using a coIP kit (Pierce). For ubiquitination assay, cells were initially lysed with RIPA buffer containing 1% SDS, the cell extracts were diluted with RIPA buffer until 0.1% SDS concentration before IP, and immunoblottings were performed as described previously (Tokunaga et al., 2009).

Confocal Microscopy

Cells grown on chamber slides were mock infected or infected with SeV for 10 hr, followed by fixation with 2% paraformaldehyde solution at room temperature for 20 min. For colocalization of TRIM25 and HOIL-1L/HOIP, mouse anti-TRIM25 (anti-EFP; BD Biosciences), rabbit anti-EFP (Santa Cruz), goat anti-HOIL-1L (anti-RBCK1; Santa Cruz), and mouse anti-HOIP (mN1) were used.

Protein Purification and In Vitro Ubiquitination Assay

TRIM25 WT was cloned into pGEX-4T-1 vector. TRIM25 $RING^{CS}$-V5, HOIL-1LΔRBR-V5, and HOIPΔRBR-Flag were cloned into pGEX-6P-1 vector. BL21 *E. coli* were transformed with each plasmid. Proteins were purified using Glutathione Sepharose4B resin according to the manufacturer's instruction. LUBAC complex, E1, and E2 proteins were purified, and in vitro ubiquitination assays were carried out as described previously (Kirisako et al., 2006). In vitro translation was performed using TnT Quick Coupled Transcription/Translation system (Promega) according to the manufacturer's instruction.

In Vitro Binding Assays

Purified GST-TRIM25 (250 ng) and GST-RIG-I-2CARD (250 ng) were incubated together with increasing amounts of purified GST-HOIL-1L ΔRBR-V5/GST-HOIPΔRBR-Flag for 2 hr at 4°C. R37 anti-RIG-I antibody was added and further incubated for 2 hr, followed by incubation with protein A/G bead for 2 hr. Samples were eluted by SDS-sample buffer and subjected to IB analysis. For TRIM25 in vitro binding to immobilized RIG-I, GST-RIG-I-2CARD were diluted in bicarbonate buffer and coated onto Maxisorb ELISA plates (200 ng/well). Biotin-labeled GST-TRIM25 was added to wells together with increasing amounts of unlabeled GST-TRIM25 or GST-HOIL-1L ΔRBR-V5/GST-HOIPΔRBR-Flag. After washing, bound TRIM25 was detected using Streptavidin-HRP.

SUPPLEMENTAL INFORMATION

Supplemental Information includes five figures and can be found with this article online at doi:10.1016/j.molcel.2010.12.029.

ACKNOWLEDGMENTS

This work was partly supported by CA082057, AI083025, AI083355, KRIBB, GRL Program (K20815000001) from National Research Foundation of Korea, Hastings Foundation, and Fletcher Jones Foundation (J.U.J.) and by AI087846-01A1 and RR00168 (M.U.G.). We thank Stacy Lee for manuscript preparation and all of J.U.J.'s lab members for their discussions.

Received: April 1, 2010
Revised: August 9, 2010
Accepted: December 14, 2010
Published: February 3, 2011

REFERENCES

Alam, S.L., Sun, J., Payne, M., Welch, B.D., Blake, B.K., Davis, D.R., Meyer, H.H., Emr, S.D., and Sundquist, W.I. (2004). Ubiquitin interactions of NZF zinc fingers. EMBO J. *23*, 1411–1421.

Arimoto, K., Takahashi, H., Hishiki, T., Konishi, H., Fujita, T., and Shimotohno, K. (2007). Negative regulation of the RIG-I signaling by the ubiquitin ligase RNF125. Proc. Natl. Acad. Sci. USA *104*, 7500–7505.

Bhoj, V.G., and Chen, Z.J. (2009). Ubiquitylation in innate and adaptive immunity. Nature *458*, 430–437.

Friedman, C.S., O'Donnell, M.A., Legarda-Addison, D., Ng, A., Cardenas, W.B., Yount, J.S., Moran, T.M., Basler, C.F., Komuro, A., Horvath, C.M., et al. (2008). The tumour suppressor CYLD is a negative regulator of RIG-I-mediated antiviral response. EMBO Rep. *9*, 930–936.

Gack, M.U., Shin, Y.C., Joo, C.H., Urano, T., Liang, C., Sun, L., Takeuchi, O., Akira, S., Chen, Z., Inoue, S., and Jung, J.U. (2007). TRIM25 RING-finger E3 ubiquitin ligase is essential for RIG-I-mediated antiviral activity. Nature *446*, 916–920.

Gack, M.U., Kirchhofer, A., Shin, Y.C., Inn, K.S., Liang, C., Cui, S., Myong, S., Ha, T., Hopfner, K.P., and Jung, J.U. (2008). Roles of RIG-I N-terminal tandem CARD and splice variant in TRIM25-mediated antiviral signal transduction. Proc. Natl. Acad. Sci. USA *105*, 16743–16748.

Gack, M.U., Albrecht, R.A., Urano, T., Inn, K.S., Huang, I.C., Carnero, E., Farzan, M., Inoue, S., Jung, J.U., and Garcia-Sastre, A. (2009). Influenza A Virus NS1 Targets the Ubiquitin Ligase TRIM25 to Evade Recognition by the Host Viral RNA Sensor RIG-I. Cell Host Microbe *5*, 439–449.

Ikeda, F., and Dikic, I. (2008). Atypical ubiquitin chains: new molecular signals. 'Protein Modifications: Beyond the Usual Suspects' review series. EMBO Rep. *9*, 536–542.

Ishikawa, H., Kato, M., Hori, H., Ishimori, K., Kirisako, T., Tokunaga, F., and Iwai, K. (2005). Involvement of heme regulatory motif in heme-mediated ubiquitination and degradation of IRP2. Mol. Cell *19*, 171–181.

Kanayama, A., Seth, R.B., Sun, L., Ea, C.K., Hong, M., Shaito, A., Chiu, Y.H., Deng, L., and Chen, Z.J. (2004). TAB2 and TAB3 activate the NF-kappaB pathway through binding to polyubiquitin chains. Mol. Cell *15*, 535–548.

Kato, H., Takeuchi, O., Sato, S., Yoneyama, M., Yamamoto, M., Matsui, K., Uematsu, S., Jung, A., Kawai, T., Ishii, K.J., et al. (2006). Differential roles of MDA5 and RIG-I helicases in the recognition of RNA viruses. Nature *441*, 101–105.

Kawai, T., and Akira, S. (2008). Toll-like receptor and RIG-I-like receptor signaling. Ann. N Y Acad. Sci. *1143*, 1–20.

Kawai, T., Takahashi, K., Sato, S., Coban, C., Kumar, H., Kato, H., Ishii, K.J., Takeuchi, O., and Akira, S. (2005). IPS-1, an adaptor triggering RIG-I- and Mda5-mediated type I interferon induction. Nat. Immunol. *6*, 981–988.

Kayagaki, N., Phung, Q., Chan, S., Chaudhari, R., Quan, C., O'Rourke, K.M., Eby, M., Pietras, E., Cheng, G., Bazan, J.F., et al. (2007). DUBA: a deubiquitinase that regulates type I interferon production. Science *318*, 1628–1632.

Kim, M.J., Hwang, S.Y., Imaizumi, T., and Yoo, J.Y. (2008). Negative feedback regulation of RIG-I-mediated antiviral signaling by interferon-induced ISG15 conjugation. J. Virol. *82*, 1474–1483.

Kirisako, T., Kamei, K., Murata, S., Kato, M., Fukumoto, H., Kanie, M., Sano, S., Tokunaga, F., Tanaka, K., and Iwai, K. (2006). A ubiquitin ligase complex assembles linear polyubiquitin chains. EMBO J. *25*, 4877–4887.

Komuro, A., and Horvath, C.M. (2006). RNA- and virus-independent inhibition of antiviral signaling by RNA helicase LGP2. J. Virol. *80*, 12332–12342.

Lin, R., Yang, L., Nakhaei, P., Sun, Q., Sharif-Askari, E., Julkunen, I., and Hiscott, J. (2006). Negative regulation of the retinoic acid-inducible gene I-induced antiviral state by the ubiquitin-editing protein A20. J. Biol. Chem. *281*, 2095–2103.

Meyer, H.H., Wang, Y., and Warren, G. (2002). Direct binding of ubiquitin conjugates by the mammalian p97 adaptor complexes, p47 and Ufd1-Npl4. EMBO J. *21*, 5645–5652.

Meylan, E., Curran, J., Hofmann, K., Moradpour, D., Binder, M., Bartenschlager, R., and Tschopp, J. (2005). Cardif is an adaptor protein in the RIG-I antiviral pathway and is targeted by hepatitis C virus. Nature *437*, 1167–1172.

Moore, C.B., Bergstralh, D.T., Duncan, J.A., Lei, Y., Morrison, T.E., Zimmermann, A.G., Accavitti-Loper, M.A., Madden, V.J., Sun, L., Ye, Z., et al. (2008). NLRX1 is a regulator of mitochondrial antiviral immunity. Nature *451*, 573–577.

Nakhaei, P., Genin, P., Civas, A., and Hiscott, J. (2009a). RIG-I-like receptors: sensing and responding to RNA virus infection. Semin. Immunol. *21*, 215–222.

Nakhaei, P., Mesplede, T., Solis, M., Sun, Q., Zhao, T., Yang, L., Chuang, T.H., Ware, C.F., Lin, R., and Hiscott, J. (2009b). The E3 ubiquitin ligase Triad3A negatively regulates the RIG-I/MAVS signaling pathway by targeting TRAF3 for degradation. PLoS Pathog. *5*, e1000650.

Pickart, C.M., and Fushman, D. (2004). Polyubiquitin chains: polymeric protein signals. Curr. Opin. Chem. Biol. *8*, 610–616.

Rahighi, S., Ikeda, F., Kawasaki, M., Akutsu, M., Suzuki, N., Kato, R., Kensche, T., Uejima, T., Bloor, S., Komander, D., et al. (2009). Specific recognition of linear ubiquitin chains by NEMO is important for NF-kappaB activation. Cell *136*, 1098–1109.

Rothenfusser, S., Goutagny, N., DiPerna, G., Gong, M., Monks, B.G., Schoenemeyer, A., Yamamoto, M., Akira, S., and Fitzgerald, K.A. (2005). The RNA helicase Lgp2 inhibits TLR-independent sensing of viral replication by retinoic acid-inducible gene-I. J. Immunol. *175*, 5260–5268.

Saitoh, T., Tun-Kyi, A., Ryo, A., Yamamoto, M., Finn, G., Fujita, T., Akira, S., Yamamoto, N., Lu, K.P., and Yamaoka, S. (2006). Negative regulation of interferon-regulatory factor 3-dependent innate antiviral response by the prolyl isomerase Pin1. Nat. Immunol. *7*, 598–605.

Seth, R.B., Sun, L., Ea, C.K., and Chen, Z.J. (2005). Identification and characterization of MAVS, a mitochondrial antiviral signaling protein that activates NF-kappaB and IRF 3. Cell *122*, 669–682.

Tian, Y., Zhang, Y., Zhong, B., Wang, Y.Y., Diao, F.C., Wang, R.P., Zhang, M., Chen, D.Y., Zhai, Z.H., and Shu, H.B. (2007). RBCK1 negatively regulates

tumor necrosis factor- and interleukin-1-triggered NF-kappaB activation by targeting TAB2/3 for degradation. J. Biol. Chem. *282*, 16776–16782.

Tokunaga, F., Sakata, S., Saeki, Y., Satomi, Y., Kirisako, T., Kamei, K., Nakagawa, T., Kato, M., Murata, S., Yamaoka, S., et al. (2009). Involvement of linear polyubiquitylation of NEMO in NF-kappaB activation. Nat. Cell Biol. *11*, 123–132.

Wang, H., Matsuzawa, A., Brown, S.A., Zhou, J., Guy, C.S., Tseng, P.H., Forbes, K., Nicholson, T.P., Sheppard, P.W., Hacker, H., et al. (2008). Analysis of nondegradative protein ubiquitylation with a monoclonal antibody specific for lysine-63-linked polyubiquitin. Proc. Natl. Acad. Sci. USA *105*, 20197–20202.

Xu, L.G., Wang, Y.Y., Han, K.J., Li, L.Y., Zhai, Z., and Shu, H.B. (2005). VISA is an adapter protein required for virus-triggered IFN-beta signaling. Mol. Cell *19*, 727–740.

Yoneyama, M., Kikuchi, M., Natsukawa, T., Shinobu, N., Imaizumi, T., Miyagishi, M., Taira, K., Akira, S., and Fujita, T. (2004). The RNA helicase RIG-I has an essential function in double-stranded RNA-induced innate antiviral responses. Nat. Immunol. *5*, 730–737.

Zeng, W., Sun, L., Jiang, X., Chen, X., Hou, F., Adhikari, A., Xu, M., and Chen, Z.J. (2010). Reconstitution of the RIG-I pathway reveals a signaling role of unanchored polyubiquitin chains in innate immunity. Cell *141*, 315–330.

Zenke-Kawasaki, Y., Dohi, Y., Katoh, Y., Ikura, T., Ikura, M., Asahara, T., Tokunaga, F., Iwai, K., and Igarashi, K. (2007). Heme induces ubiquitination and degradation of the transcription factor Bach1. Mol. Cell. Biol. *27*, 6962–6971.

Zhang, M., Tian, Y., Wang, R.P., Gao, D., Zhang, Y., Diao, F.C., Chen, D.Y., Zhai, Z.H., and Shu, H.B. (2008). Negative feedback regulation of cellular antiviral signaling by RBCK1-mediated degradation of IRF3. Cell Res. *18*, 1096–1104.

Zhao, S., and Ulrich, H.D. (2010). Distinct consequences of posttranslational modification by linear versus K63-linked polyubiquitin chains. Proc. Natl. Acad. Sci. USA *107*, 7704–7709.